Pre-publication and Peer-reviewed copy: Sazia Iftekhar, Madeleine Rauhauser, Benjamin D. Hage, and David S. Hage, "Determination of Binding Constants by Ultrafast Affinity Extraction: Theoretical and Experimental Studies of Optimum Conditions for Analysis", J. Chromatogr. A, 1707 (2023) 464307. (doi: 10.1016/j.chroma.2023.464307)

Determination of Binding Constants by Ultrafast Affinity Extraction: Theoretical and Experimental Studies of Optimum Conditions for Analysis

Sazia Iftekhar[a], Madeleine Rauhauser[a], Benjamin D. Hage[b], and David S. Hage[a*]

[a]Department of Chemistry, University of Nebraska-Lincoln

[b]Department of Biological Systems Engineering, University of Nebraska-Lincoln

*Author for Correspondence: Chemistry Department, University of Nebraska-Lincoln, Lincoln, NE 68588-0304, USA. Phone: 402-472-2744; Email: dhage1@unl.edu

Abstract

Ultrafast affinity extraction (UAE) is a form of microscale affinity HPLC that can be employed to quickly measure equilibrium constants for solute-binding agent interactions in solution. This study used chromatographic and equilibrium theory with universal plots to examine the general conditions that are needed in UAE to obtain accurate, precise, and robust measurements of equilibrium constants for such interactions. The predicted results were compared to those obtained by UAE in studies that examined the binding of various drugs with two transport proteins: human serum albumin and α_1-acid glycoprotein. The most precise and robust conditions for these binding studies occurred for systems with intermediate values for their equilibrium free fraction for the solute ($F_0 \approx 0.20$-0.80). These trends showed good agreement with those seen in prior studies using UAE. It was further determined how the apparent free fraction of a solute was related to the dissociation rate of this solute, the time allowed for solute dissociation during UAE, and the equilibrium free fraction for the solute. These results also agreed with experimental results, as obtained for the binding of warfarin and gliclazide with human serum albumin. The final section examined how a change in the apparent free fraction, as caused by solute dissociation, affected the accuracy of an equilibrium constant that was measured by UAE. In addition, theoretical plots were generated to allow the selection of conditions for UAE that provided a given level of accuracy during the measurement of an equilibrium constant. The equations created and trends identified for UAE were general ones that can be extended in future work to other solutes and binding agents.

Keywords: Ultrafast affinity extraction; Drug-protein binding; Free drug fraction; Association equilibrium constant; Affinity microcolumn

1. Introduction

Ultrafast affinity extraction (UAE) is a form of affinity chromatography and microscale HPLC that can be employed to directly examine, in solution, the binding of solutes with agents in systems with weak-to-strong reversible interactions [1–4]. This technique involves introducing a solution-phase mixture of a solute and binding agent into an affinity microcolumn, which contains a selective capture agent for the solute and has a volume in the mid-to-low microliter range (see Figure 1) [1,5,6]. When this solute-binding agent mixture is applied to the microcolumn under conditions that produce a small column residence time, a portion of the free (or non-bound) form of the solute can be captured without significant release of more solute from the soluble binding agent. Measurement of the free solute fraction under these conditions can be used to determine the equilibrium constant for the interaction of the solute and binding agent in the original sample [2,7–12]. However, if a longer column residence time is employed (e.g., through use of a lower flow rate), some of the solute may dissociate from its binding agent during passage of the sample through the microcolumn. This, in turn, can lead to an increase in the apparent free fraction that is measured for the solute and an error in the estimated equilibrium constant if such dissociation is not considered [4,7,8,10].

UAE has several advantages compared to other techniques for characterizing solute interactions with binding agents. These advantages include its fast analysis times, which are usually on the order of only a few minutes; its need for only small sample volumes (i.e., a few μL); and its ability to be used with systems covering a broad range of affinities (i.e., association equilibrium constants spanning from at least 10^4-10^9 M^{-1}) [2,9–13]. In addition, UAE is a label-free technique and does not require immobilization or modification of either the solute or binding agent in the sample [1,4]. However, preliminary studies are often currently required in UAE to

determine the flow rate, column size, and sample concentrations that should be used with new solutes and binding agents to obtain accurate equilibrium constants [1–4,7,10]. In addition, a better understanding is needed of how changing the conditions used in UAE may affect the accuracy, precision, and robustness of this method, such as when it is used to obtain the equilibrium constant for an interaction between a given solute and binding agent.

This study will first examine the general conditions, as determined from chromatographic and equilibrium theory, that are needed in UAE to provide robust and precise measurements of equilibrium constants for solutes and binding agents in solution-phase samples. These conditions will be compared to those that have been used in previous UAE studies of drug interactions with the serum transport proteins human serum albumin (HSA) [4,8,10,11,13] and α_1-acid glycoprotein (AGP) [9,12]. The predicted and observed effects of solute dissociation from its binding agent during UAE will also be examined with respect to the relative change that this process may produce in the apparent free fraction for a solute. In addition, this work will consider the effect of such a change in the measured free fraction on the accuracy of equilibrium constant measurements by UAE. The results from these studies will be used to identify general conditions for UAE that can be used in future studies to obtain accurate, robust, and precise measurements of equilibrium constants for the interactions of other solutes and binding agents.

2. Experimental

2.1. Reagents

The racemic warfarin (≥ 98% pure), HSA (Cohn fraction V, essentially fatty acid-free, ≥ 96% pure), and gliclazide (≥ 98%) used to obtain new data for this study were obtained from Sigma Aldrich (St. Louis, MO, USA). Nucleosil Si-300 silica (300 Å pore size; 7 µm particle diameter) was purchased from Macherey Nagel (Dűren, Germany). Water from a Milli-Q system (EMD

Millipore Sigma, Burlington, MA) was utilized to prepare the drug solutions, drug/protein mixtures, and buffers used in this study. The buffers were passed through Osmonics 0.22 μm GNWP nylon membrane filters from Fisher Scientific (Pittsburgh, PA, USA). Reagents for the micro bicinchoninic acid (BCA) protein assay were obtained from Pierce (Rockford, IL, USA).

2.2. Instrumentation

A Prep 24 pump from ChromTech (Apple Valley, MN, USA) was used to pack the microcolumns employed in acquiring experimental data for Sections 3.3-3.4. UAE studies were carried out with a HPLC system that consisted of an AS-2057 autosampler, a UV-2075 absorbance detector, and a PU-2080 Plus pump from Jasco (Easton, MD, USA). An X-LC 3167CO column oven from Jasco was used to maintain a temperature of 37.0 (± 0.1) ºC during each analysis. A six-port LabPro valve (Rheodyne, Cotati, CA, USA) was also utilized as part of this system. The HPLC system was controlled by LCNet and ChromNAV v1.18.04 software from Jasco.

2.3. Chromatographic studies and preparation of affinity microcolumns

The Schiff base method was utilized to place HSA onto a silica support for acquiring the experimental data in Sections 3.3-3.4 [4,8,14]. A control support was prepared in the same manner but without the addition of HSA. The protein content of the HSA support was determined in triplicate by using a micro BCA assay, with HSA being employed as the calibration standard and the control support as the blank. The HSA content for the supports used in the UAE studies with warfarin and gliclazide were 81.0 (± 4.0) and 79.0 (± 10.0) mg HSA/g silica, respectively, where the values in parentheses represent a range of ± 1 S.D. Each HSA support or control support was packed into a stainless steel microcolumn with a length of 10 mm and an inner diameter (i.d.) of 2.1 mm. These microcolumns were downward slurry packed using pH 7.4, 0.067 M potassium

phosphate buffer that was applied at a pressure of 28 MPa (4000 psi). The supports and microcolumns were stored at 4.0 ℃ in the same pH 7.4 buffer when not in use.

A pH 7.4, 0.067 M potassium phosphate buffer was utilized as both the mobile phase in the UAE studies and to prepare the drug and protein solutions that were used as the injected samples in Sections 3.3-3.4. Prior to use, this mobile phase was degassed for ~30 min. The drug and drug-HSA samples were preheated to a temperature of 37.0 (± 0.1) ℃ for at least 30 min in the autosampler before injection. The microcolumns were equilibrated with pH 7.4, 0.067 M potassium phosphate buffer at 0.50 mL/min in a column oven at 37.0 (± 0.1) ℃ for 30-60 min prior to sample injection. The free fraction of each drug was measured by injecting 10 μM of the drug without HSA (i.e., as a standard), followed by a mixture containing 10 μM of the drug plus 20 μM HSA. The injection volumes and detection wavelengths were as follows: warfarin, 20 μL and 308 nm; gliclazide, 10 μL and 226 nm. All samples were injected in replicate (n = 5) at flow rates ranging from 0.5 mL/min up to ~2.25-3.0 mL/min. The equilibrium free fraction (F_0) of each drug was estimated by examining the fit of the measured free fractions vs flow rate and from data collected at the highest tested flow rates [1,4]. Baseline correction and analysis of the chromatograms were done using the progressive, linear and exponentially modified Gaussian (EMG) functions, respectively, of PeakFit v4.12 (Jandel Scientific, San Rafael, CA, USA). Additional data analysis was performed using Excel for Office 365 (Microsoft, Redmond, WA, USA).

Prior experimental data, as used in Sections 3.1-3.2, were obtained from Refs. [4,8-10,12,13]. These data were for UAE studies with various drugs and normal or glycated HSA in buffered solutions or serum [4,8,10,13] and UAE binding studies for drugs with AGP in pooled serum or serum collected from individuals with systemic lupus erythematosus (SLE) [9,12]. The

studies of drug-HSA binding in buffered solutions employed single-column UAE systems and the following conditions: column dimensions, 1.0-10.0 mm × 2.1 mm i.d.; equilibrium free fraction (F_0) range, 0.14-0.69; and ratio of total concentrations of drug and protein (C_D/C_P), 0.50-1.00 [4,8,10]. Drug-HSA binding in serum was examined using two-column UAE systems under the following conditions: 1st column dimensions, 1.0-10.0 mm × 2.1 mm i.d.; 2nd column dimensions, 10.0-25.0 mm × 2.1 mm i.d.; F_0 range, 0.007-0.095; and estimated C_D/C_P ratio, 0.006-0.56 [13]. Drug-AGP binding in serum was examined by using two-column UAE systems under the following conditions: 1st column dimensions, 2.0-5.0 mm × 2.1 mm i.d.; 2nd column dimensions, 5.0-10.0 mm × 2.1 mm i.d.; F_0 range, 0.019-0.29; and estimated C_D/C_P ratio, 0.011-0.77 [9,12].

3. Results and Discussion

3.1. Determination of association constant from original free fraction of a solute

The first part of this study examined the conditions that are needed in UAE to obtain a robust estimate of an equilibrium constant for a solute or drug (D) with a soluble binding agent or protein (P) in an injected sample. This type of analysis is carried out by using data from UAE to measure or estimate the free (non-bound) fraction of the solute at equilibrium in the sample; this value is represented by the solute's original free fraction, F_0. This information can be acquired by injecting the solute-binding agent mixture onto an affinity microcolumn under flow rate and column size conditions that provide a column residence time sufficiently small to minimize any appreciable dissociation of the solute from its binding agent as the sample passes through the microcolumn [1,4]. The value of F_0 that is obtained by UAE under these conditions can then be used along with the known total concentration of the solute or drug (C_D) and the total concentration of binding agent or protein in the original sample (C_P) to determine the association equilibrium constant (K_a) for the solute with the binding agent. The relationship between K_a and F_0 for a solute

and binding agent with a 1:1 interaction is shown in eq. (1) [1,15] (see Supplemental Material for derivation).

$$K_a = \frac{(1-F_0)}{F_0 C_P\left(1-\frac{C_D}{C_P}+\frac{C_D}{C_P}F_0\right)} \quad (1)$$

The above equation can also be written in terms of the dissociation equilibrium constant (K_d) for the solute and binding agent, by using the fact that $K_a = 1/K_d$.

Similar expressions to eq. (1) can be derived for more complex systems. For example, a related expression can be written for a binding agent that has *n* independent sites for D, and that is examined with an excess of P versus D, as can be accomplished by using the global affinity constant nK'_a instead of K_a. In this case, nK'_a is an overall apparent equilibrium constant that is equal to the term $\Sigma n_i K_{ai}$, where n_i is the relative amount of site i that is present (in moles site i per moles P) and K_{ai} is the association equilibrium constant of this site for D [1,16,17]. If *n* sites are present that all have approximately the same association equilibrium constant, nK'_a converts to the simpler term nK_a, which can also be used in place of K_a in eq. (1) [16-18].

The relationship in eq. (1) can be rearranged to produce a more general and universal expression that is based on only dimensionless parameters. This can be done by revising eq. (1) to now use the product $K_a C_P$ as the dependent variable (i.e., a term that has no units if K_a is expressed in M^{-1} and C_P has units of M). This modification results in the revised relationship that is provided in eq. (2) (Note: An equivalent expression in terms of K_d can be obtained by replacing $K_a C_P$ with C_P/K_d or in terms of nK'_a by replacing $K_a C_P$ with $nK'_a C_P$).

$$K_a C_P = \left(\frac{1-F_0}{F_0}\right)\left(\frac{1}{1-\frac{C_D}{C_P}+\frac{C_D}{C_P}F_0}\right) \quad (2)$$

Along with $K_a C_P$, all terms in this equation are now dimensionless, including the original solute free fraction (F_0) and the ratio C_D/C_P (e.g., when C_D and C_P are both expressed in equivalent units

such as molarity). As an alternative, eq. (2) can be written in a form in which the base-10 logarithm is taken of both sides of this expression, giving the result shown in eq. (3).

$$\log(K_a C_P) = \log\left(\frac{1-F_0}{F_0}\right) - \log\left(1 - \frac{C_D}{C_P} + \frac{C_D}{C_P} F_0\right) \quad (3)$$

In this report, these universal relationships are used to see how the product $K_a C_P$ will vary as the values of F_0 and C_D/C_P are altered within a sample to be examined by UAE. This will be done to see what general types of experimental conditions (e.g., ratios for C_D/C_P and relative size of C_P vs K_a) are needed in UAE when determining the value of K_a from F_0 for systems with various binding strengths.

The relationships between the terms in eqs. (2) and (3) are illustrated in Figure 2, which shows plots of $\log(K_a C_p)$ vs F_0 and C_D/C_P. A base-10 log scale for $K_a C_p$ is used in these plots to provide a more convenient examination of the results over a broad range of values in this combined term. Figure 2 also focuses on the relationship between $K_a C_P$ and F_0 or C_D/C_P for systems in which the ratio C_D/C_P is 1.00 or less, which represents the conditions that have been used in prior work with UAE for binding studies [4,8,9,10,12,13]. Plots made in Figure 2(a) at C_D/C_P ratios below 0.10 give a similar response to the one seen at $C_D/C_P = 0.10$, due to convergence of the results at low values for C_D/C_P, as is further illustrated in Figure 2(b).

Figure 2(a) shows that the conditions used in UAE for binding studies can be grouped into three general domains in terms of the value for F_0. First, there is a set of conditions that occur when a small value of F_0 is present (i.e., roughly $F_0 \leq 0.20$). Under these conditions, there is a large increase in $\log(K_a C_P)$ as F_0 is decreased, with this change becoming more pronounced as C_D/C_P increases to 1.00. Second, there is a group of conditions that occur over an intermediate region of F_0 values, which span from approximately $F_0 \approx 0.20$-0.80 for all the values of C_D/C_P shown in Figure 2(a). In this range, there is a more gradual and almost linear change in $\log(K_a C_P)$

vs F_0 at all values for C_D/C_P. This range also has a small increase in $\log(K_a C_P)$ as C_D/C_P increases to 1.00, although the extent of this change is not as large as it is in the first general domain. Third, there is a set of conditions that occur when $F_0 \geq 0.80$, in which the value of $\log(K_a C_P)$ has a sharp decrease as F_0 approaches 1.00. In this range, the value for $\log(K_a C_P)$ at all C_D/C_P ratios approaches the same result as F_0 is increased to 1.00.

The effect of changing C_D/C_P on $\log(K_a C_P)$, as shown in Figure 2(b), is generally much less than the effect of varying F_0. However, the value of $\log(K_a C_P)$ does tend to increase, at least slightly, as the value of C_D/C_P is raised from a small ratio (i.e., a representing a large excess of P versus D) to 1.00 (i.e., equal total concentrations of D and P). One consequence of this trend is that the use in UAE of a C_D/C_P ratio that is at or near 1.00 will generally provide a broader range of $\log(K_a C_P)$ and $K_a C_P$ values that fall within the desired range of $F_0 \approx 0.20$-0.80 when compared to working at a lower C_D/C_P ratio (e.g., $C_D/C_P = 0.10$). This means the higher C_D/C_P ratios that are shown in Figure 2(b) will generally provide more robust conditions for the determination of K_a than the use of lower C_D/C_P ratios.

One way the plots in Figure 2 can be used is to determine which combinations of F_0 and C_D/C_P will provide the most robust estimates of K_a in UAE. These conditions occur in the second and intermediate region in Figure 2(a), at F_0 values of roughly 0.20-0.80 and which give a gradual change in the value of $\log(K_a C_P)$ vs F_0. This range for F_0 corresponds in Figure 2(a) to $\log(K_a C_P)$ values that span from around -0.51 to 1.30 (or $K_a C_P$ = 0.31-20) at a C_D/C_P ratio of 1.00 and -0.59 to 0.64 ($K_a C_P$ = 0.26-4.4) at a C_D/C_P ratio of 0.10. These results indicate using a C_D/C_P ratio of 1.00 will provide around a 3.8-fold broader range in $K_a C_P$ values that fall within the desired range of $F_0 \approx 0.20$-0.80 when compared to working at a C_D/C_P ratio of 0.10. At the center of the central

range in Figure 2(a) (i.e., at $F_0 = 0.5$), the value of $\log(K_a C_P)$ spans from roughly 0.00 to 0.30 (or $K_a C_P \approx 1.0$ to 2.0) in going from a low ratio of C_D/C_P to $C_D/C_P = 1.00$.

To illustrate how these relationships might be used in experimental design, one can begin with a rough estimate of K_a for the desired system. This estimate might be obtained from the literature for similar interactions or through a preliminary measurement using UAE or another method to determine binding constants (e.g., ultrafiltration, equilibrium dialysis, or various separation- or spectroscopic-based techniques) [1,16,17,19]. This initial estimate can then be used with eq. (2) and Figure 2 to determine which conditions will provide the most robust and reliable measurement of K_a in more detailed studies. For example, a solute and binding agent with an expected K_a of 1.0×10^6 M^{-1} will give a value of $K_a C_P = 2.0$ when used with a total binding agent concentration (C_P) of 2.0×10^{-6} M. When this binding agent is used with an equivalent total solute or drug concentration ($C_D = 2.0 \times 10^{-6}$ M, giving $C_D/C_P = 1.00$), this combination of conditions should provide a value for F_0 of 0.50, which is in the center of the desired range in Figure 2(a) for robust equilibrium constant measurements by UAE. In the same manner, systems with initial estimated values for K_a of 1.0×10^4 M^{-1} or 1.0×10^5 M^{-1} will have values of $K_a C_P = 2.0$ when the total binding agent concentration is 2.0×10^{-4} M or 2.0×10^{-5} M, respectively; when an equivalent drug concentration is used (i.e., $C_D/C_P = 1.00$), this combination of conditions will again produce a value for F_0 of 0.50 that is in the center of the optimum range for K_a measurements in Figure 2(a).

In work with biological matrices and other real samples, it is possible the values of C_D/C_P and K_a that are present may result in F_0 values that are outside of the optimum, intermediate range in Figure 2(a). For instance, some mixtures of solutes and binding agents may have a high value for $\log(K_a C_P)$ and strong binding, which can give F_0 values below 0.20. Figure 2(a) shows that

the measurement of K_a under such conditions is possible but will be more sensitive than the central region of this plot to variations in the values for F_0 or C_D/C_P. At the other extreme are conditions that create weak binding and a high value for F_0 (> 0.80). Work under these conditions is not affected as much by changes in C_D/C_P as in the left and central regions in Figure 2(a); however, estimates made of K_a in this domain will be highly sensitive to moderate or even small changes in F_0. Thus, careful control of the experimental conditions is needed in UAE when working under conditions that produce either low or high values for F_0.

The theoretical results in Figure 2 were compared to conditions that have been used for UAE in prior binding studies with various drugs and HSA or AGP [4,8-10,12,13]. Figure 3 shows the conditions and results that have been obtained for 16 drug-protein combinations in buffered solutions using HSA or modified forms of this protein (see Supplemental Material for further details) [4,8,10]. These studies were conducted with mixtures that had a value for C_D/C_P of 0.50 or 1.00 and which resulted in values for F_0 of ~0.14-0.70. This range of conditions showed good agreement with those present in the intermediate range of Figure 2(a). The values that were obtained for K_a in these systems ranged from ~6×10^4 to 2×10^6 M^{-1}, with $\log(K_a C_P)$ spanning from 0.09 to 1.04 at $C_D/C_P = 0.50$ and from -0.19 to 1.32 at $C_D/C_P = 1.00$ [4,8,10].

Figure 4 provides a similar comparison between the behavior that is predicted by eqs. (2-3) and conditions used in previous UAE studies that have measured binding constants by solutes with HSA or AGP in serum (i.e., a situation in which the values of C_P and C_D/C_P are determined by the sample content). The experimental data in Figure 4 were obtained for 13 drugs at typical therapeutic concentrations in serum and with HSA or AGP at normal or disease state concentrations (i.e., a total of 30 drug/protein combinations) [9,12,13]. The range of F_0 values that were measured with these samples spanned from 0.007 to 0.29. The drugs and proteins used in

these studies had values for K_a that ranged from ~2×10^4 to 2×10^6 M^{-1} and log($K_a C_P$) values that spanned from roughly 0.6 to 2.2 [9,12,13]. The C_D/C_P ratios that were present in these samples were estimated to range from 0.01 to 0.77. Although the F_0 values that were measured in these studies were well below the optimum central range of 0.20-0.80 in Figure 2(a), it was still possible to use data under these conditions to determine K_a by UAE [9,12,13].

3.2. Relationship of precision in F_0 to precision in K_a

The next group of factors that were considered in selecting conditions for binding studies in UAE were those that affect the precision of K_a, as obtained from the measured free fraction under equilibrium conditions, F_0. These factors were evaluated by utilizing error propagation, with the initial assumption that the precision of K_a was determined mainly by the uncertainty in the measured value of F_0 instead of the much lower uncertainties expected for C_D and C_P. The basis for this assumption was the relatively high precision (i.e., often at least ± 0.1-1%) that is typically present in a modern chemical analysis for mass and volume measurements during the preparation of samples and reagents [20]. The Supplemental Material contains a further discussion of this assumption and its validity, including a mathematical description of the expected contributions to the precision of K_a by the uncertainties in C_D and C_P.

It was found through error propagation, and with the assumption that the measurement of F_0 was the main contribution to the uncertainty in K_a, that both the absolute and relative precisions in the measured value of F_0 (as described by S_{F_0} and S_{F_0}/F_0, respectively) are related to the relative precision in the calculated value of K_a. These relationships are given in eqs. (4-5) (see Supplemental Material for derivations), where S_{K_a} is the absolute standard deviation for K_a, and the relative precision in K_a is represented by the ratio S_{K_a}/K_a.

$$\frac{S_{K_a}}{K_a} \approx \left(S_{F_0}\right)\left(\frac{1}{(1-F_0)} + \frac{1}{F_0} + \frac{\left(\frac{C_D}{C_P}\right)}{\left(1-\frac{C_D}{C_P}+\frac{C_D}{C_P}F_0\right)}\right) \quad (4)$$

$$\frac{S_{K_a}}{K_a} \approx \left(\frac{S_{F_0}}{F_0}\right)\left(\frac{F_0}{(1-F_0)} + 1 + \frac{F_0\left(\frac{C_D}{C_P}\right)}{\left(1-\frac{C_D}{C_P}+\frac{C_D}{C_P}F_0\right)}\right) \quad (5)$$

Both eqs. (4) and (5) are general expressions based on the dimensionless parameters F_0 and C_D/C_P. Related expressions can be written through the same process in terms of a dissociation equilibrium constant, K_d, and its standard deviation, S_{K_d}, or a global affinity constant, nK'_a, and its standard deviation, $S_{nK'_a}$. In addition, eqs. (4) and (5) can be rearranged into eqs. (6) and (7), respectively, to directly compare the relative precision for K_a to the absolute and relative precisions for F_0 under various experimental conditions.

$$\left(\frac{S_{K_a}}{K_a}\right)/\left(S_{F_0}\right) \approx \left(\frac{1}{(1-F_0)} + \frac{1}{F_0} + \frac{\left(\frac{C_D}{C_P}\right)}{\left(1-\frac{C_D}{C_P}+\frac{C_D}{C_P}F_0\right)}\right) \quad (6)$$

$$\left(\frac{S_{K_a}}{K_a}\right)/\left(\frac{S_{F_0}}{F_0}\right) \approx \left(\frac{F_0}{(1-F_0)} + 1 + \frac{F_0\left(\frac{C_D}{C_P}\right)}{\left(1-\frac{C_D}{C_P}+\frac{C_D}{C_P}F_0\right)}\right) \quad (7)$$

Figure 5(a) was generated by using eq. (6) to see how the how the ratio $(S_{K_a}/K_a)/S_{F_0}$ (i.e., the relative precision for K_a compared to the absolute precision in F_0) changes as F_0 is varied for solute-binding agent systems in which the concentration ratio C_D/C_P is less than or equal to 1.00. This figure indicates that the best relative precision in the measurement of K_a is obtained for F_0 values in the range of roughly 0.20-0.80, with a minimum occurring at $F_0 \approx 0.50$-0.60. The smallest values for $(S_{K_a}/K_a)/S_{F_0}$ under these conditions approach 4.0 at low C_D/C_P ratios. As F_0 decreases below 0.20 or increases above 0.80, the term $(S_{K_a}/K_a)/S_{F_0}$ increases to a value of ≥ 6.4 at a C_D/C_P ratio of 0.10 and to even higher values as C_D/C_P approaches 1.00. The dependence of this precision term on C_D/C_P becomes larger at small F_0 values, while the dependence on C_D/C_P becomes small and essentially negligible as F_0 approaches 1.00.

Figure 5(b) was prepared in a similar manner by using eq. (7) to see how the relative precision for K_a vs the relative precision for F_0, as given by the ratio $(S_{K_a}/K_a)/(S_{F_0}/F_0)$, was affected by a change in F_0 at C_D/C_P values of 1.00 or less. The ratio of these relative precisions has a gradual decrease as F_0 nears 0.00, while the same ratio shows a large increase when F_0 is raised above 0.80. The smallest value that can be obtained for $(S_{K_a}/K_a)/(S_{F_0}/F_0)$ is around 1.0, as is approached when F_0 is 0.20 or less and C_D/C_P is at or below 0.10. At the same low values for F_0, the ratio of relative precisions for K_a vs F_0 is approximately 2.0 at $C_D/C_P = 1.00$.

Several practical factors regarding experimental design in UAE for binding studies can be obtained from Figures 5(a-b). One observation is that the lowest relative precision that can be obtained for K_a will be a value for (S_{K_a}/K_a) that is about four times the absolute precision (S_{F_0}) and one- to two-times the relative precision (S_{F_0}/F_0) in the corresponding value of F_0 that was used to calculate K_a. The relationships between (S_{K_a}/K_a) and (S_{F_0}) or (S_{F_0}/F_0) in eqs. (4-5) further indicate that obtaining a more precise estimate of F_0 will always lead to a proportional improvement in the relative precision of K_a. In addition, the use of a small C_D/C_P ratio will result in a better relative precision for K_a than when using a C_D/C_P ratio that is near or equal to 1.00.

It was further noted that many of the trends in Figures 5(a-b) follow the same pattern seen in Figure 2(a) for determining the most robust conditions for UAE in binding studies. For instance, the increase in Figures 5(a-b) as F_0 approaches 1.00 for the relative precision of K_a versus either the absolute or relative precision in F_0 reflects the greater uncertainty that is present when high values of F_0 are used to estimate an equilibrium constant. The increase in Figure 5(a) for (S_{K_a}/K_a) versus the absolute precision of F_0 as F_0 is decreased towards 0.00 is also similar to the behavior seen in Figure 2(a) and reflects the greater uncertainty that is present when low values of F_0 are used to estimate K_a. Figures 2(a) and 5(a) have the same intermediate range ($F_0 \approx 0.20$-0.80) that

provides the most robust or precise estimate of K_a. The upper end of this range ($F_0 \approx 0.80$) further agrees with the range of F_0 values that provides the lowest ratios for the relative precision for K_a vs the relative precision of F_0 in Figure 5(b). Although this ratio of relative precisions reaches a lower limit as F_0 approaches 0.00 in Figure 5(b), F_0 values of roughly 0.20 or lower are the same conditions under which contributions to the uncertainty in K_a may increase due to the uncertainty in C_D or C_P (see Supplemental Material). This again makes the intermediate F_0 range of ≈ 0.20-0.80 the conditions most likely to provide both a robust and precise estimate for K_a.

A comparison was next made between Figures 5(a-b) and 2(a-b) for the effects of a change in C_D/C_P on the relative precision vs robustness for a measurement of K_a. In all these plots, the largest dependence of the results on C_D/C_P occurred at small F_0 values. Each of these plots also had essentially the same result at C_D/C_P ratios of 0.10-1.00 as the value of F_0 increased to 1.00. One important difference between Figures 5(a-b) and 2(a-b) was in the general range of C_D/C_P ratios that provided the best results. For instance, in Figures 2(a-b) a C_D/C_P ratio of 1.00 gave the most robust conditions for determining K_a, as discussed in Section 3.1; however, in Figures 5(a-b), low C_D/C_P ratios gave the best relative precision in K_a. These trends suggest a C_D/C_P ratio of 1.00 may work best when UAE is to be used in an initial screening study to estimate K_a. If desired, the optimum conditions identified from the screening study can then be adjusted to conduct work at a lower C_D/C_P ratio to provide a more precise estimate of K_a.

Figures 6(a) and 6(b) show values for the absolute precision S_{F0} and the relative precision S_{F0}/F_0 that have been obtained by UAE during the measurement of F_0 in binding studies for drugs with HSA or AGP (i.e., as used in Figures 3-4 and that employed either simple mixtures or serum samples) [4,8–10,12,13]. Figure 6(a) indicates that a much broader range in S_{F0} values was generally obtained as F_0 increased in these experiments, while a broader range in S_{F0}/F_0 tended to

occur in Figure 6(b) as F_0 decreased. Mixtures of drugs with HSA in buffer gave values for F_0 of ~0.14 to 0.70 at C_D/C_P ratios of 0.50 or 1.00 [4,8,10]; these conditions resulted in S_{F0} values spanning from ± 0.01-0.07 and relative precisions for F_0 (as given by the ratio S_{F0}/F_0) of ± 0.02-0.21 (or ± 2-21%). Work with serum, which had lower C_D/C_P ratios and typically produced smaller values for F_0, also tended to give smaller values for S_{F0} and a slightly larger set of values for S_{F0}/F_0. These latter studies had S_{F0} values that ranged from ± 0.001 to 0.027 and S_{F0}/F_0 ratios that spanned from ± 0.01-0.28 (i.e., relative precisions of ± 1-28%), as acquired for drugs and samples with F_0 values of 0.0069 to 0.29 and C_D/C_P ratios of 0.006 to 0.77 [9,12,13].

The ratios of (S_{Ka}/K_a) vs S_{Fo} and S_{F0}/F_0 that were obtained in these experiments were compared with the values predicted by chromatographic and equilibrium theory, as represented by eqs. (4-5) or (6-7). This comparison is shown in Figures 7(a) and 7(b). Good agreement was seen in the predicted and observed values or trends when using UAE with either simple solute-protein mixtures or serum. For example, in Figure 7(a) the lowest values of $(S_{Ka}/K_a)/S_{Fo}$ were obtained at F_0 values of 0.20 and up to values of at least 0.70 in this set of experimental results. In addition, the value of $(S_{Ka}/K_a)/S_{Fo}$ over this range in F_0 approached a minimum of around 4.0 at low values of C_D/C_P. As F_0 decreased below 0.20, there was an increase in the experimental values for $(S_{Ka}/K_a)/S_{Fo}$ that became especially steep as F_0 decreased below 0.05. In Figure 7(b), the lowest values of $(S_{Ka}/K_a)/(S_{Fo}/F_0)$ were seen as F_0 was decreased, approaching upper and lower limits spanning from roughly 1.0 to 2.0 as C_D/C_P was raised from a small ratio up to 1.00. These combined results confirmed that the most precise estimates of K_a were obtained over a broad range of intermediate values for F_0 (i.e., experimentally from 0.20 up to at least 0.70). The good agreement between the experimental data and trends in Figure 7(b) also confirmed the assumption made in eqs. (4-7) that the uncertainty in F_0, rather than the uncertainties in C_D and C_P, was the

main factor the determined the overall uncertainty in K_a during these studies (see Supplemental Material for further discussion).

3.3. Effect of solute dissociation on measured free fractions in UAE

It is known in UAE that using medium-to-long residence times for a sample in a microcolumn can lead to dissociation of a solute from its soluble binding agent [4,7,8,10]. This, in turn, will result in an increase in the apparent, measured free fraction of the solute (F_t) when compared to the free fraction that would be expected in the sample at equilibrium (F_0). If the apparent free fraction is then used to estimate the equilibrium constant for the solute and binding agent, this may produce a systematic error in the estimated constant. This section will examine the general factors that lead to a change in F_t vs F_0, along with the relative size of this change under various operating conditions in UAE.

It has been shown previously that solute dissociation from its soluble binding can be described by a pseudo first-order dissociation rate process on the time scale of a typical UAE experiment [1,4]. In this model, it is assumed that the solute in its free form is captured immediately by the microcolumn used in UAE and that no reassociation of the solute with its soluble binding agent occurs as the sample passes through this microcolumn [1,4]. Under these conditions, the extent of solute dissociation will depend on the residence time for the sample in the microcolumn (t) and the dissociation rate constant of the solute from its binding agent (k_d). The amount of solute that can dissociate will also be determined by the size of the original free fraction of the solute at equilibrium (F_0). The relationship between these parameters and the observed free fraction for the solute (F_t) is described by eq. (8).

$$F_t = F_0 + (1 - F_0)(1 - e^{-k_d t}) \quad (8)$$

If both sides of eq. (8) are divided by F_0, the following equivalent relationship is produced that is expressed in terms of the relative size of F_t vs F_0, as given by the ratio F_t/F_0.

$$\frac{F_t}{F_0} = 1 + (\frac{1}{F_0} - 1)\,(1 - e^{-k_d\,t}) \qquad (9)$$

Eq. (9) now provides a way of generating universal plots that look at the effect on F_t/F_0 when varying the product $k_d\,t$ (i.e., which will be a unitless parameter when k_d and t are in the same units of time) and the original free fraction for the solute at equilibrium, F_0.

Figure 8 gives some universal plots based on eq. (9) that show how the ratio F_t/F_0 varies with the product $k_d\,t$ and over F_0 values ranging from 0.1 to 0.9. These results indicate that the deviation of F_t from F_0 will increase with an increase in $k_d\,t$, as will occur as either the size of the dissociation rate constant increases (i.e., faster solute dissociation is present) or the column residence time for the sample increases (i.e., more time is allowed for dissociation). The size of this deviation will become more pronounced as the value of F_0 becomes smaller, which is a situation in which more solute is initially present in a bound form in the sample and is potentially available for dissociation (Note: The maximum value for F_t/F_0 in each case is equal to $1/F_0$). The extent of the deviation in F_t vs F_0 can become particularly important for systems with moderate-to-high levels of binding (i.e., $F_0 \leq 0.5$) and with fast dissociation and/or long column residence times (i.e., moderate-to-high values of $k_d\,t$). For instance, in a system with a high level of initial binding and a value for F_0 of 0.10, there will be only about a 1.18-fold difference in F_t vs F_0 at a $k_d\,t$ value of 0.02 but a 4.5-fold difference at a higher $k_d\,t$ value of 0.5. On the other hand, in a system with only a small level of initial solute binding and an F_0 value of 0.90, the difference in F_t vs F_0 at $k_d\,t = 0.02$ and 0.5 will be only 0.22% and 4.4%, respectively.

These predicted trends were next compared to data that were obtained by UAE over a comparable range of $k_d\,t$ for two experimental systems: the binding of HSA to the drugs warfarin

and gliclazide. These two drugs were selected as models because they both have well-characterized binding to HSA and have been previously examined by UAE [1,21]. In addition, the binding or rate constants for these systems are typical of those seen for drug interactions with serum protein such as HSA [1,4,8-10,12,13,21], with warfarin/HSA being an example of a system with a single major site of interaction and gliclazide/HSA representing a system with multiple binding sites [1,21]. The fits between the experimental and predicted results are shown in Figure 9. The ranges of column residence times that were present during these experiments with HSA and warfarin or gliclazide were 0.67-3.33 s and 0.83-3.33 s, respectively. The estimated values of K_a and k_d for the warfarin/HSA system were ~2-3 × 10^5 M^{-1} and 0.4-0.6 s^{-1}, while the corresponding values for the gliclazide/HSA system were ~1 × 10^5 M^{-1} and 0.5-0.6 s^{-1} [1,21].

Both systems in Figure 9 gave good agreement between the experimental results and the changes in F_t/F_0 vs k_d t that were predicted by eq. (9), with correlation coefficients of 0.902-0.982 (n = 4). In these two cases, the warfarin/HSA system, which had the lower value for F_0 (≈ 0.20), gave a larger deviation in F_t vs F_0 than the gliclazide/HSA system (for which F_0 ≈ 0.40). For instance, the predicted deviation in F_t vs F_0 was 1.9- and 2.6-fold for warfarin and HSA under conditions that gave k_d t values of around 0.25 and 0.50, while the same conditions for k_d t gave deviations of 1.3- and 1.6-fold in F_t vs F_0 when examining the binding of gliclazide with HSA by UAE. To evaluate these effects for other systems and by using similar plots, an initial estimate of k_d, as well as F_t and F_0 at known values of t, can be obtained by UAE using techniques such as the two-flow rate method described in Ref. [8].

3.4. Effect of solute dissociation on estimates of equilibrium constants by UAE

This section examined how differences between the true free fraction of a solute in a sample at equilibrium (F_0) and the apparent free fraction (F_t, as measured at column residence time t)

affected the accuracy of an equilibrium constant that was determined by UAE. This was done by describing the apparent association equilibrium constant ($K_{a,app}$) in a similar manner to that was used for the true value of K_a in eq. (1), but now using F_t in place of F_0. This results in the following equation that relates $K_{a,app}$ to F_t and the ratio C_D/C_P.

$$K_{a,app} = \frac{(1-F_t)}{F_t C_P\left(1-\frac{C_D}{C_P}+\frac{C_D}{C_P}F_t\right)} \tag{10}$$

Equivalent relationships can be written for an apparent dissociation equilibrium constant ($K_{d,app}$) that is measured by UAE, by substituting $1/K_{d,app}$ for $K_{a,app}$ in eq. (10), or for an apparent global affinity constant ($nK'_{a,app}$), by substituting $nK'_{a,app}$ for $K_{a,app}$ [1,11,13].

It was shown in the last section that the value of F_t in UAE will always be greater than or equal to F_0. This means the value of $K_{a,app}$ should always be less than or equal to K_a (or that $K_{d,app}$ will be greater than or equal to K_d). The relative value of $K_{a,app}$ vs K_a, which represents the difference in these values and the error obtained when using $K_{a,app}$ in place of K_a to describe solute binding, can be obtained by dividing eq. (10) by eq. (1). The new expression that is obtained for the ratio $K_{a,app}/K_a$ is given in eq. (11) (see Supplemental Material for derivation; the equivalent expression in terms of dissociation equilibrium constants is obtained by replacing $K_{a,app}/K_a$ with $K_d/K_{d,app}$).

$$\frac{K_{a,app}}{K_a} = \left(\frac{F_0}{F_t}\right)\left[\frac{1-F_0\left(\frac{F_t}{F_0}\right)}{\left(1-\frac{C_D}{C_P}+\frac{C_D}{C_P}F_0\left\{\frac{F_t}{F_0}\right\}\right)}\right] \Big/ \left[\frac{1-F_0}{\left(1-\frac{C_D}{C_P}+\frac{C_D}{C_P}F_0\right)}\right] \tag{11}$$

This expression again contains only ratios and dimensionless parameters, making it possible to use eq. (11) to generate universal plots to see how the ratio of $K_{a,app}$ vs K_a changes as a function of F_0, and as the ratios F_t/F_0 or C_D/C_P vary for a solute and binding agent that are examined by UAE.

By using eq. (11), a set of universal plots were generated in Figure 10 that show how $K_{a,app}$ compares to the true value of K_a as the size of F_t is varied vs F_0. These plots also show how the change in $K_{a,app}/K_a$ vs F_t/F_0 is altered by using various ratios of C_D/C_P in UAE. The *x*-axis in these plots extends over values for F_t/F_0 that range from 1.0 to $1/F_0$, with the latter being the highest ratio for F_t/F_0 at a given F_0 that will provide a value for $K_{a,app}$ that is greater than or equal to 0. In all these plots, the ratio $K_{a,app}/K_a$ decreases from a maximum value of 1.0 as the ratio F_t/F_0 is increased above one. As noted earlier, this means $K_{a,app}$ will always be smaller than K_a when solute dissociation occurs in UAE and causes F_t to be greater than F_0.

The plots in Figure 10 are for F_0 values of 0.20, 0.40, 0.60, and 0.80. It can be seen by comparing these plots that the use of a smaller ratio for C_D/C_P will result in smaller deviations in $K_{a,app}$ vs K_a, with this effect becoming larger as the value of F_0 is decreased. Furthermore, the decrease in $K_{a,app}/K_a$ occurs over a broader range of F_t/F_0 values as F_0 is decreased. For instance, in Figure 10(a) and at an F_0 value of 0.20, a 19% increase in F_t vs F_0 results in a ~20% deviation in $K_{a,app}$ vs K_a at $C_D/C_P = 0.10$. In Figure 10(d) only a 4% increase in F_t vs F_0 produced the same degree of error in K_a at $F_0 = 0.80$ and $C_D/C_P = 0.10$.

Figure 11 shows some experimental data and plots for $K_{a,app}/K_a$ vs F_t/F_0 that were constructed using UAE data for the binding of warfarin or gliclazide with HSA in buffer. The values of F_0 in these systems were 0.20 for warfarin/HSA and 0.40 for gliclazide/HSA. These experimental results gave good agreement with the behavior predicted by eq. (11), with absolute values for their correlation coefficients of 0.921-0.969 (n = 5). Both the experimental models showed the expected decrease in $K_{a,app}$ vs K_a as F_t was increased compared to F_0. Furthermore, the system with the smaller value for F_0 (i.e., the warfarin/HSA mixture) had this change in $K_{a,app}$ occur over a broader total range of values for F_t/F_0. These trends agreed with the predicted

behavior from Figure 10. Similar plots can be generated for other systems by using initial estimates of F_t and F_0 that are obtained by UAE at two or more known column residence times and flow rates by using methods such as those described in Refs. [1,8].

Eq. (11) was also used to see which values of F_t/F_0 were needed at specific combinations of F_0 and C_D/C_P to produce a given difference between $K_{a,app}$ and K_a. The results are shown in Figure 12. As was suggested in Figure 10, the use of low C_D/C_P ratios gave experimental conditions in which a particular deviation of F_t from F_0 had the smallest effect on the difference between $K_{a,app}$ and K_a. This trend held at all values for F_0 and resulted in similar behavior for systems with C_D/C_P ratios of around 0.50 or lower, as shown in Figure 12(a-d). At C_D/C_P ratios above this range, the deviation in $K_{a,app}$ vs K_a became more pronounced at a given value for F_t/F_0 and the range of F_t/F_0 over which these deviations occurred became narrower, as can be seen by comparing Figures 12(a-c) and 12(d-f). These plots also make it possible to identify the experimental conditions and combinations of F_t/F_0, F_0, and C_D/C_P that should be used to keep the difference between $K_{a,app}$ and K_a within a given range. For instance, if up to a 20% error is to be allowed in $K_{a,app}$ vs K_a for a system in which the binding conditions result in $F_0 = 0.20$ and $C_D/C_P = 0.10$, conditions for UAE should be selected that provide a value for F_t/F_0 of about 1.2 or less. A similar approach can be used to identify conditions to select F_0, C_D/C_P, and F_t/F_0 values that will provide other maximum differences between $K_{a,app}$ and K_a.

4. Conclusion

This study employed chromatographic and equilibrium theory to determine the conditions that are needed in UAE to obtain accurate, precise, and robust estimates of equilibrium constants between solutes and their binding agents. Factors considered were the original free solute fraction at equilibrium (F_0), the relative concentration of the solute compared to its binding agent (C_D/C_P),

and the relative size of the expected association equilibrium constant vs the total concentration of binding agent ($K_a C_P$). The precision of the measured free fraction and the effects of differences in the apparent solute free fraction (F_t) vs F_0 due to solute dissociation were also considered.

General equations and universal plots were produced to examine the relationship between $K_a C_P$, C_D/C_P, and F_0 and to determine which values for these factors provided the most robust estimates of K_a during UAE. Related equations were derived to show how these parameters affected the relative precision obtained in the calculated value for K_a. It was found that solute and binding agent combinations with F_0 values in the range of 0.20 to 0.80 produced both the most robust and precise estimates of K_a at typical C_D/C_P ratios that have been used in UAE for binding studies. A pseudo-first order kinetic model was used to produce an equation and universal plots to describe how solute dissociation from its binding agent in a sample affected the apparent free fraction for a solute when compared to the true value at equilibrium. In addition, plots were generated to allow the selection of conditions, such as the amount of solute vs binding agent and equilibrium free solute fraction, that will provide a desired level of accuracy during the measurement of equilibrium constants by UAE.

The equations and plots that were created in this study, and the trends that were identified, are general ones that can be extended in the future to the analysis of new solutes and binding agents by UAE. For instance, these tools should now make it possible to predict and more easily select conditions that will allow the estimation of equilibrium constants by UAE for a variety of systems, including the interactions of drugs, hormones, environmental contaminants, and other classes of solutes with either natural or synthetic binding agents [4,5]. This ability, in turn, should greatly expand the applicability of UAE in such fields as clinical chemistry and biomedical research, as well as materials science and environmental studies [1–5].

5. Acknowledgments

This work was supported by the National Science Foundation Division of Chemistry under grant CMI 2108881. The authors have no conflicts of interest to declare for this work.

6. References

[1] S.R. Beeram, X. Zheng, K. Suh, D.S. Hage, Characterization of solution-phase drug-protein interactions by ultrafast affinity extraction, Methods 146 (2018) 46–57.

[2] X. Zheng, C. Bi, M. Brooks, D.S. Hage, Analysis of hormone-protein binding in solution by ultrafast affinity extraction: interactions of testosterone with human serum albumin and sex hormone binding globulin, Anal. Chem. 87 (2015) 11187–11194.

[3] M.P. Czub, B.S. Venkataramany, K.A. Majorek, K.B. Handing, P.J. Porebski, S.R. Beeram, K. Suh, A.G. Woolfork, D.S. Hage, I.G. Shabalin, W. Minor, Testosterone meets albumin-the molecular mechanism of sex hormone transport by serum albumins, Chem. Sci. 10 (2019) 1607–1618.

[4] X. Zheng, Z. Li, M.I. Podariu, D.S. Hage, Determination of rate constants and equilibrium constants for solution-phase drug-protein interactions by ultrafast affinity extraction, Anal. Chem. 86 (2014) 6454–6460.

[5] E.L. Rodriguez, S. Poddar, S. Iftekhar, K. Suh, A.G. Woolfork, S. Ovbude, A. Pekarek, M. Walters, S. Lott, D.S. Hage, Affinity chromatography: a review of trends and developments over the past 50 years, J. Chromatogr. B 1157 (2020) 122332.

[6] X. Zheng, Z. Li, S. Beeram, R. Matsuda, E.L. Pfaunmiller, M. Podariu, C.J. White II, N. Carter, D.S. Hage, Analysis of biomolecular interactions using affinity microcolumns: a review, J. Chromatogr. B 968 (2014) 49-63.

[7] S. Beeram, C. Bi, X. Zheng, D.S. Hage, Chromatographic studies of drug interactions with

alpha$_1$-acid glycoprotein by ultrafast affinity extraction and peak profiling, J. Chromatogr. A 1497 (2017) 92–101.

[8] S. Iftekhar, D.S. Hage, Evaluation of microcolumn stability in ultrafast affinity extraction for binding and rate studies, J. Chromatogr. B 1187 (2021) 123047.

[9] C. Bi, X. Zheng, D.S. Hage, Analysis of free drug fractions in serum by ultrafast affinity extraction and two-dimensional affinity chromatography using α_1-acid glycoprotein microcolumns, J. Chromatogr. A 1432 (2016) 49–57.

[10] B. Yang, X. Zheng, D.S. Hage, Binding studies based on ultrafast affinity extraction and single- or two-column systems: interactions of second- and third-generation sulfonylurea drugs with normal or glycated human serum albumin, J. Chromatogr. B 1102–1103 (2018) 8–16.

[11] X. Zheng, R. Matsuda, D.S. Hage, Analysis of free drug fractions by ultrafast affinity extraction: interactions of sulfonylurea drugs with normal or glycated human serum albumin, J. Chromatogr. A 1371 (2014) 82–89.

[12] S.R. Beeram, C. Zhang, K. Suh, W.A. Clarke, D.S. Hage, Characterization of drug binding with alpha$_1$-acid glycoprotein in clinical samples using ultrafast affinity extraction, J. Chromatogr. A 1649 (2021) 462240.

[13] X. Zheng, M. Podariu, R. Matsuda, D.S. Hage, Analysis of free drug fractions in human serum by ultrafast affinity extraction and two-dimensional affinity chromatography, Anal. Bioanal. Chem. 408 (2016) 131–140.

[14] H.S. Kim, D.S. Hage, Immobilization methods for affinity chromatography, in: D.S. Hage (Ed.), Handbook of Affinity Chromatography, 2nd ed., CRC Press, Boca Raton, FL, 2005: pp. 36–78.

[15] R. Mallik, M.J. Yoo, C.J. Briscoe, D.S. Hage, Analysis of drug-protein binding by ultrafast affinity chromatography using immobilized human serum albumin, J. Chromatogr. A 1217 (2010) 2796–2803.

[16] B. Sebille, R. Zini, C.V. Madjar, N. Thaud, J.P. Tillement, Separation procedures used to reveal and follow drug-protein binding, J. Chromatogr. 531 (1990) 51-77.

[17] D.S. Hage, S.A. Tweed, Recent advances in chromatographic and electrophoretic methods for the study of drug-protein interactions, J. Chromatogr. B 699 (1997) 499-525.

[18] G. Scatchard, The attractions of proteins for small molecules and ions, Ann. N.Y. Acad. Sci. 51 (1949) 660-672.

[19] K. Vuignier, J. Schappler, J.-L. Veuthey, P.-A. Carrupt, S. Martel, Drug–protein binding: a critical review of analytical tools, Anal. Bioanal. Chem. 398 (2010) 53–66.

[20] D.S. Hage, J.D. Carr, Analytical Chemistry and Quantitative Analysis, Prentice Hall, New York, 2011.

[21] M.J. Yoo, D.S. Hage, Use of peak decay analysis and affinity microcolumns containing silica monoliths for rapid determination of drug-protein dissociation rates, J. Chromatogr. A, 1218 (2011) 2072-2078.

Figure Legends

Figure 1. Scheme for using ultrafast affinity extraction to study binding of a solute (e.g., a drug) with a soluble binding agent (e.g., a protein) by utilizing an affinity microcolumn with a selective capture agent for the solute. The top chromatograms show data obtained for the solute and solute plus binding agent at a short column residence time and high flow rate, which are conditions that should result in little or no solute dissociation from its soluble binding agent as these agents pass through the microcolumn. These conditions provide a captured free fraction that can be used to determine the original free fraction (F_0) of the solute in its mixture with the binding agent. The bottom chromatograms show data for the same samples when they are injected at a slower flow rate and longer column residence time, giving an apparent free fraction (F_t) for the solute that is now larger than F_0. These data were acquired in pH 7.4, 0.067 M potassium phosphate buffer and at 37 °C for 20 μL injections of the drug warfarin (10 μM) in the presence or absence of the protein human serum albumin (HSA, 20 μM). These samples were injected onto a 10 mm × 2.1 mm i.d. HSA microcolumn at (top) 3.0 mL/min or (bottom) 2.0 mL/min. Other conditions are given in Section 2.3.

Figure 2. Effects of changes in the free fraction at equilibrium (F_0) and the ratio of the total concentrations for a drug/solute (D) and protein/binding agent (P) on the value of $\log(K_a C_P)$. The term $\log(K_a C_P)$ in these plots is the base-10 logarithm of the product of the association equilibrium constant (K_a) for the binding of D with P and the total concentration of the protein/binding agent (C_P). These plots were generated using eq. (2). The plots in (a) show how $\log(K_a C_P)$ changes over a given range of F_0 values and at various ratios for the total concentrations of the drug vs binding agent (C_D/C_P). The

complementary plots in (b) show how log($K_a C_P$) changes over a given range of ratios for C_D/C_P and at various values of F_0. The solid and dashed sloping lines in (a) represent the results predicted for C_D/C_P ratios ranging from 0.10 to 1.00, in increments of 0.10; the two vertical dashed lines included in this plot at $F_0 = 0.20$ and 0.80 are provided for reference. The solid and dashed sloping lines in (b) show the results predicted for F_0 values ranging from 0.10 to 0.90, in increments of 0.10.

Figure 3. Relationship between F_0 and the value of log($K_a C_P$) for several solute-binding agent systems, as illustrated with experimental data obtained by UAE for various drugs in presence of simple buffered solutions containing known amounts of normal human serum albumin (HSA) or glycated HSA (GHSA1 and GHSA2). The data points represented as squares were obtained when using a C_D/C_P ratio of 0.50 during the experiments, while the data points represented by the diamonds were obtained by using a C_D/C_P ratio of 1.00. The F_0, C_D/C_P, and K_a values for these experimental systems are provided in the Supplemental Material and are based on data obtained from Refs. [4,8,10]. The dashed lines are provided for reference and show the predicted change in log($K_a C_P$) vs F_0 at specific C_D/C_P values, as determined by using eq. (2).

Figure 4. Relationship between F_0 and the value of log($K_a C_P$) for solute-binding systems in serum samples examined by UAE. These experimental results are for drugs in the presence of (a) HSA in pooled normal serum or pooled diabetic serum or (b) AGP in pooled normal serum or serum from individuals with systemic lupus erythematosus (SLE). The F_0, C_D/C_P, and K_a values for these drug-protein systems are provided in

the Supplemental Material and are based on data obtained from Refs. [9,12,13]. The solid lines are provided for reference and show the predicted change, as based on eq. (2), in $\log(K_a C_P)$ vs F_0 at the following C_D/C_P values (listed in order from bottom-to-top): (a) 0.01, 0.05, 0.20, 0.40, and 0.60; or (b) 0.01, 0.05, 0.10, 0.20, 0.40, and 0.80.

Figure 5. Effect of varying F_0 on the relative precision of K_a, or (S_{Ka}/K_a), vs (a) the absolute precision of F_0, as represented by the ratio $(S_{Ka}/K_a)/S_{F0}$, and determined by using eq. (6) or (b) the relative precision of F_0, or (S_{F0}/F_0), as represented by the ratio $(S_{Ka}/K_a)/(S_{F0}/F_0)$ and determined by using eq. (7). The solid and dashed lines in (a) represent the results obtained by eq. (6) at C_D/C_P ratios spanning from 0.10 to 1.00, in increments of 0.10, and the inset in (a) shows an expanded view of the theoretical results that were obtained for F_0 values spanning from 0.20 to 0.80. The solid and dashed lines in (b) represent the results obtained by eq. (7) at C_D/C_P ratios ranging from 0.10 to 1.00; the inset in (b) shows an expanded view of the theoretical results that were obtained for F_0 values spanning from 0.00 to 0.80 and at C_D/C_P ratios (from bottom-to-top) of 0.10, 0.30, 0.50, 0.70, 0.90, and 1.00.

Figure 6. Measured values for (a) the absolute precision of F_0 (i.e., S_{F0}) and (b) the relative precision of F_0 (i.e., S_{F0}/F_0) as acquired for various drug-protein systems. The diamonds represent the results obtained for binding of drugs to HSA in buffer (i.e., normal or glycated HSA), the squares represent the binding of drugs to HSA in serum (i.e., pooled serum from healthy individuals or diabetic patients), and the circles represent the binding of drugs to AGP in serum (i.e., AGP in pooled normal serum or individual serum samples from individuals with SLE). The values of F_0, C_D/C_P, and

K_a, as well as the precisions, for these systems are provided in the Supplemental Material and are based on data obtained from Refs. [4,8–10,12,13].

Figure 7. Effect of F_0 on the relative precision of K_a, or (S_{Ka}/K_a), when compared to (a) the absolute precision of F_0, as represented by S_{F0}, or (b) the relative precision of F_0, as represented by S_{F0}/F_0, for data obtained in prior studies examining the binding of various drug-protein systems. The diamonds represent the results obtained for the binding of drugs to HSA in buffer (i.e., normal or glycated HSA), the squares represent the binding of drugs to HSA in serum (i.e., pooled serum from healthy individuals or diabetic patients), and the circles represent the binding of drugs to AGP in serum (i.e., AGP in pooled normal serum or individual serum samples from individuals with SLE). The error bars represent a range of ± 1 S.D. for 3-5 sample injections. The F_0, C_D/C_P, and K_a values for these systems are provided in the Supplemental Material and are based on data obtained from Refs. [4,8–10,12,13]. The solid and dashed lines in (a) and (b) represent the results obtained at C_D/C_P ratios (from bottom-to-top) of 0.006, 0.011, 0.50, 0.56, 0.77, and 1.00 (i.e., the range of C_D/C_P ratios estimated to be present in the given set of experiments). Some expanded views of (a) are provided in the Supplemental Material.

Figure 8. Relationship between F_t/F_0 and $k_d\,t$, as predicted according to eq. (9). The solid and dashed lines represent the results obtained at F_0 values ranging from 0.10 to 0.90, in increments of 0.10.

Figure 9. Relationship between F_t/F_0 and $k_d t$ for data acquired by UAE examining the binding of HSA in buffered samples with the drugs (a) warfarin and (b) gliclazide. The experimental conditions and approximate best-fit values used for warfarin were as follows: $F_0 \approx 0.20$, $C_D/C_P = 0.50$, $C_P = 20 \times 10^{-6}$ M; flow rates, 0.5-2.5 mL/min; microcolumn size, 10 mm × 2.1 mm i.d.; and $k_d \approx 0.45$ s^{-1}. The conditions used in the studies for gliclazide were as follows: $F_0 \approx 0.40$, $C_D/C_P = 0.50$, $C_P = 20 \times 10^{-6}$ M; flow rates, 0.5-2.0 mL/min; microcolumn size, 10 mm × 2.1 mm i.d.; and $k_d \approx 0.55$ s^{-1}. These results were obtained in the presence of pH 7.4, 0.067 M potassium phosphate buffer and at 37.0 (± 0.1) ℃. The error bars for F_t/F_0 represent a range of ± 1 S.D. (*n* = 5 injections), as determined through error propagation from the separate precisions for F_t and F_0. The dashed lines show the results predicted under the same conditions by using eq. (9).

Figure 10. Effect of the relative size of F_t vs F_0, as given by the ratio F_t/F_0, on the deviation of $K_{a,app}$ from K_a (or $K_{a,app}/K_a$) at various values for C_D/C_P. This set of plots show the results predicted by eq. (11) at F_0 values of (a) 0.20, (b) 0.40, (c) 0.60, and (d) 0.80. The solid and dashed lines in each figure represent the results obtained for C_D/C_P ratios ranging from 0.10 to 1.00, in increments of 0.10.

Figure 11. Effect of the relative size of F_t vs F_0, as given by the ratio of F_t/F_0, on the observed deviation of $K_{a,app}$ from K_a (or $K_{a,app}/K_a$) for mixtures of the drugs (a) warfarin and (b) gliclazide with HSA in buffered solutions. The sample, mobile phase, and column conditions were the same as in Figure 9, with results being shown for flow rates of 0.5-3.0 mL/min and $F_0 \approx 0.20$ for warfarin or 0.5-2.25 mL/min and $F_0 \approx 0.40$ for

gliclazide. The vertical error bars represent a range of ± 1 S.D. (n = 5 injections) in the calculated values of $K_{a,app}/K_a$, as found through error propagation. The dashed lines represent the results that were predicted under the same conditions when using eq. (11).

Figure 12. Relationship between the relative size of F_t vs F_0, as given the ratio F_t/F_0, with F_0 at various values for the ratio $K_{a,app}/K_a$. These plots show the results predicted by eq. (11) at C_D/C_P ratios of (a) 0.10, (b) 0.25, (c) 0.50, (d) 0.75, (e) 0.90, and (f) 1.00. The solid and dashed lines in each figure represent (from right-to-left) the results obtained for $K_{a,app}/K_a$ ratios of 0.50 to 0.95, in increments of 0.05.

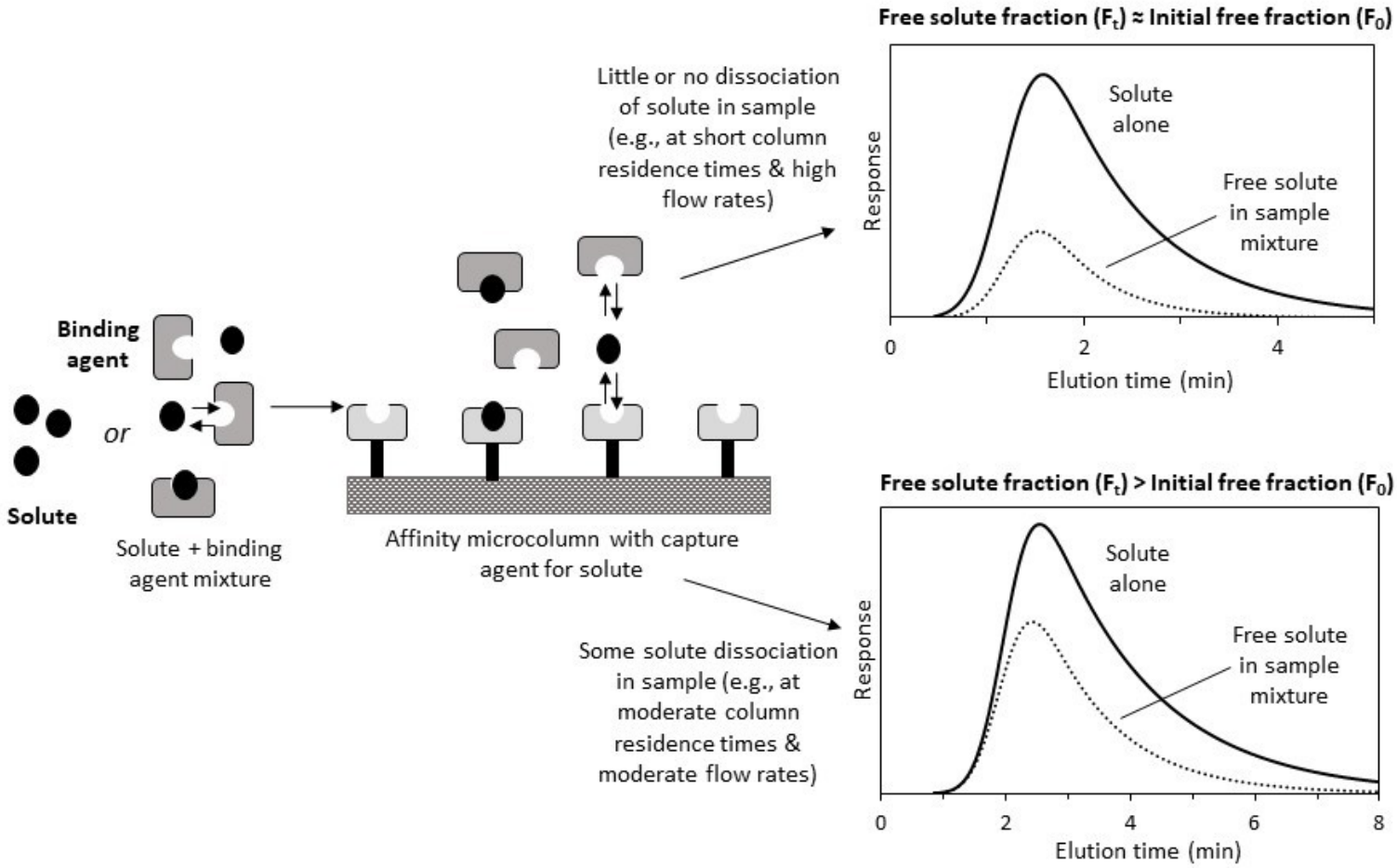
Free solute fraction (F_t) ≈ Initial free fraction (F_0)
Little or no dissociation of solute in sample (e.g., at short column residence times & high flow rates)
Solute alone
Free solute in sample mixture
Response
0
2
4
Elution time (min)
Binding agent
or
Solute
Solute + binding agent mixture
Affinity microcolumn with capture agent for solute
Free solute fraction (F_t) > Initial free fraction (F_0)
Some solute dissociation in sample (e.g., at moderate column residence times & moderate flow rates)
Solute alone
Free solute in sample mixture
Response
0
2
4
6
8
Elution time (min)

Figure 1

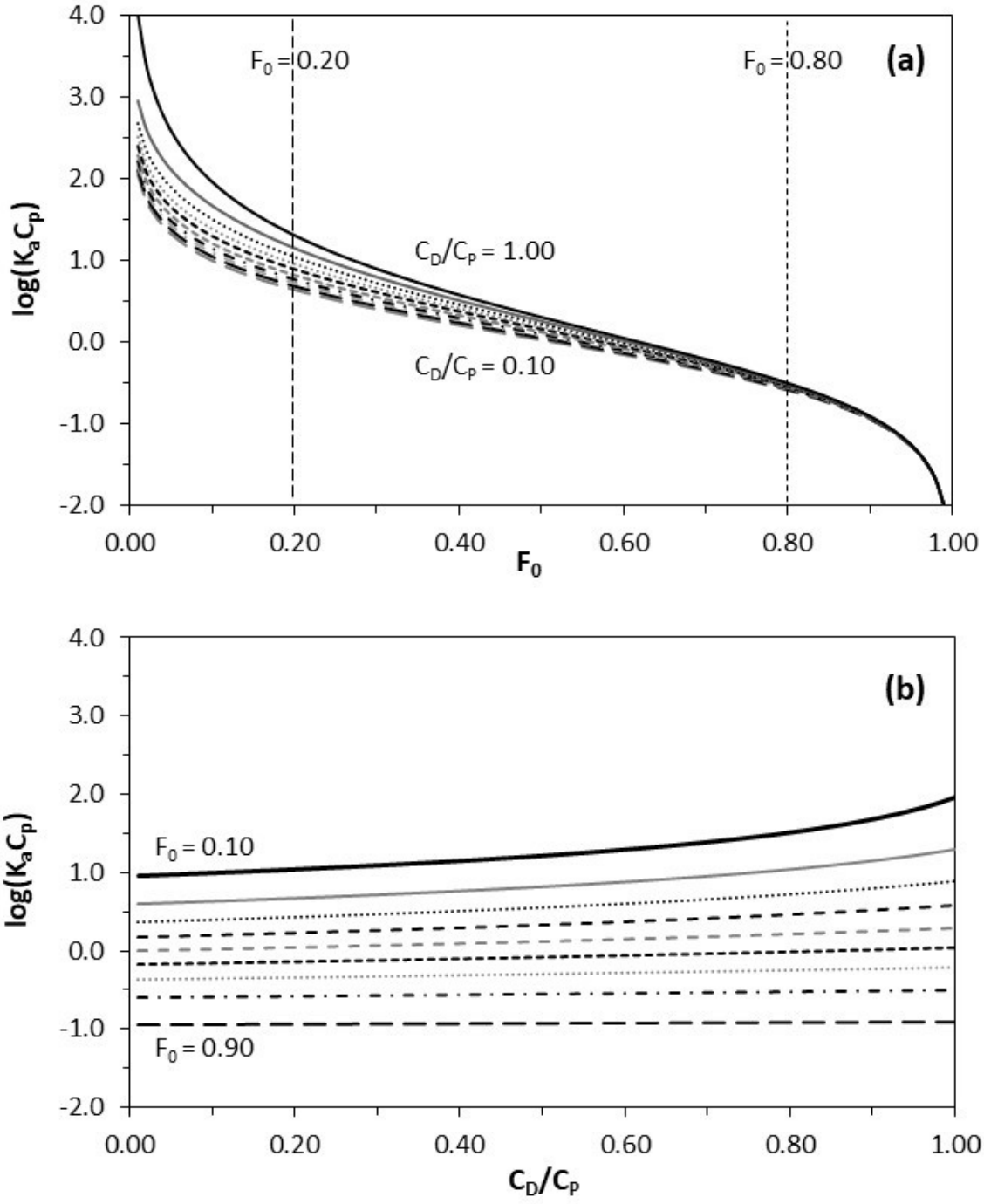
(a)
F_0 = 0.20
F_0 = 0.80
C_D/C_P = 1.00
C_D/C_P = 0.10
log(K_aC_p)
F_0
(b)
F_0 = 0.10
F_0 = 0.90
log(K_aC_p)
C_D/C_P

Figure 2

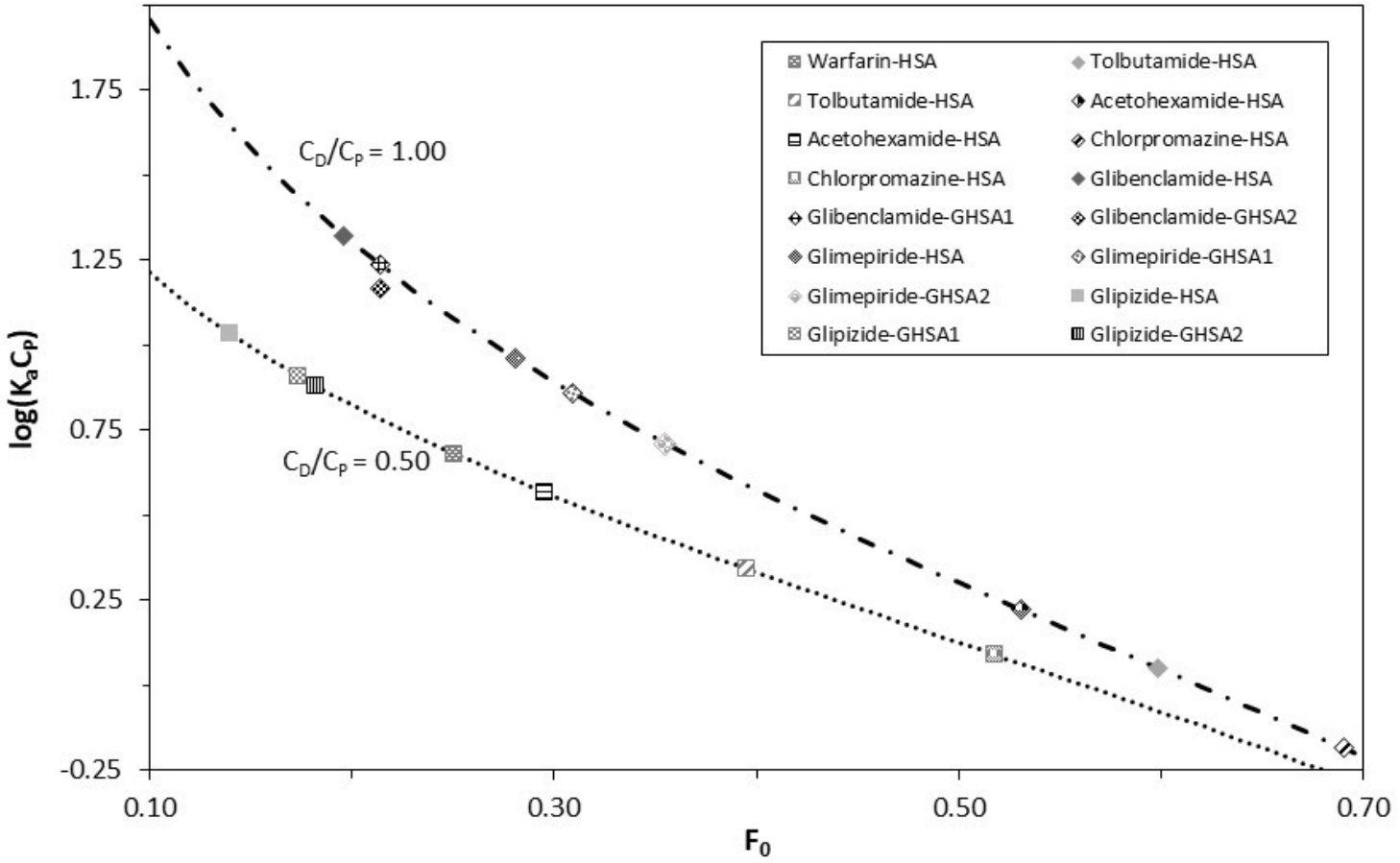
Warfarin-HSA
Tolbutamide-HSA
Tolbutamide-HSA
Acetohexamide-HSA
Acetohexamide-HSA
Chlorpromazine-HSA
Chlorpromazine-HSA
Glibenclamide-HSA
Glibenclamide-GHSA1
Glibenclamide-GHSA2
Glimepiride-HSA
Glimepiride-GHSA1
Glimepiride-GHSA2
Glipizide-HSA
Glipizide-GHSA1
Glipizide-GHSA2
$C_D/C_P = 1.00$
$C_D/C_P = 0.50$
$\log(K_a C_P)$
F_0
1.75
1.25
0.75
0.25
-0.25
0.10
0.30
0.50
0.70

Figure 3

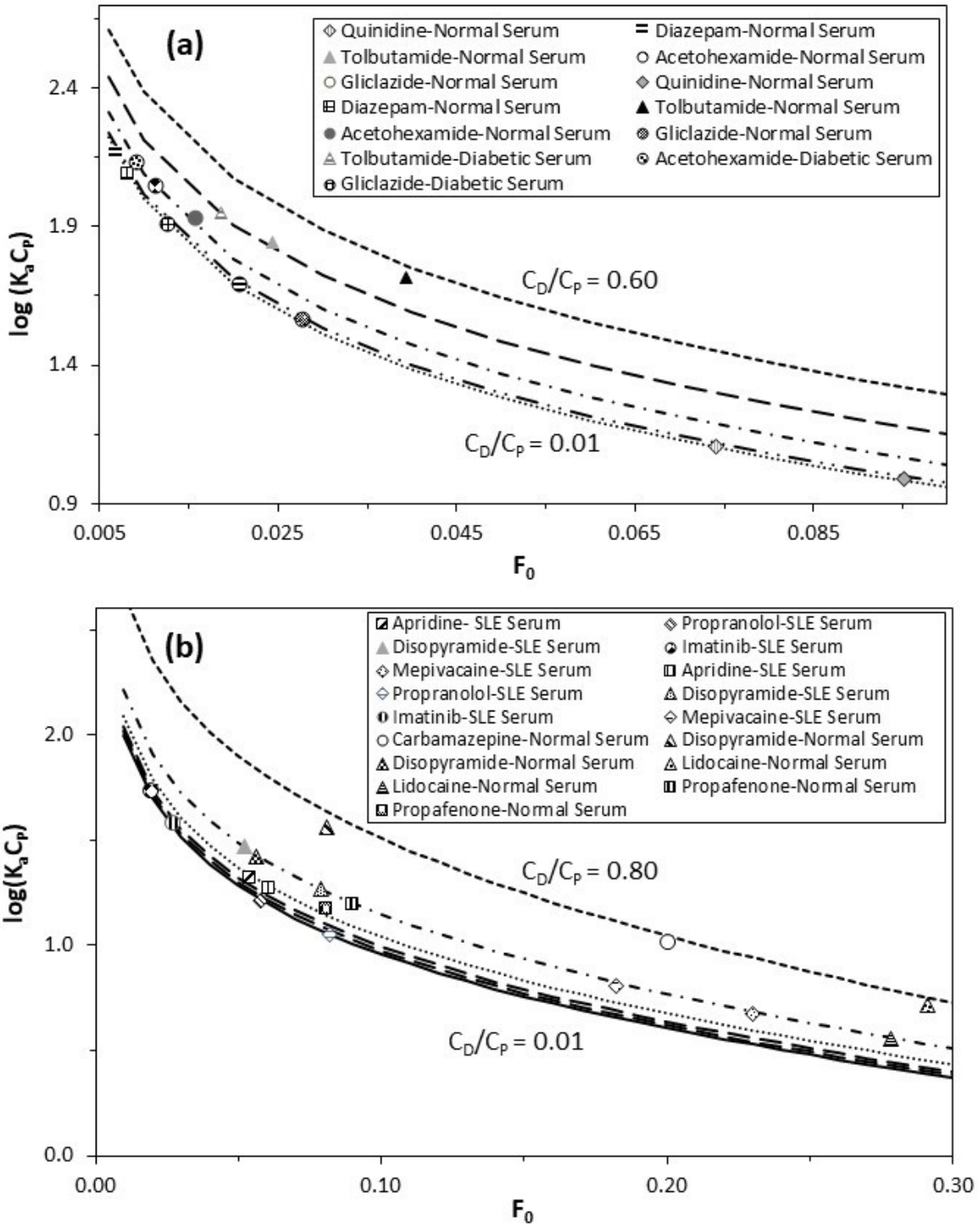
(a)
Quinidine-Normal Serum
Diazepam-Normal Serum
Tolbutamide-Normal Serum
Acetohexamide-Normal Serum
Gliclazide-Normal Serum
Quinidine-Normal Serum
Diazepam-Normal Serum
Tolbutamide-Normal Serum
Acetohexamide-Normal Serum
Gliclazide-Normal Serum
Tolbutamide-Diabetic Serum
Acetohexamide-Diabetic Serum
Gliclazide-Diabetic Serum
C_D/C_P = 0.60
C_D/C_P = 0.01
log (K_aC_P)
F_0
(b)
Apridine- SLE Serum
Propranolol-SLE Serum
Disopyramide-SLE Serum
Imatinib-SLE Serum
Mepivacaine-SLE Serum
Apridine-SLE Serum
Propranolol-SLE Serum
Disopyramide-SLE Serum
Imatinib-SLE Serum
Mepivacaine-SLE Serum
Carbamazepine-Normal Serum
Disopyramide-Normal Serum
Disopyramide-Normal Serum
Lidocaine-Normal Serum
Lidocaine-Normal Serum
Propafenone-Normal Serum
Propafenone-Normal Serum
C_D/C_P = 0.80
C_D/C_P = 0.01
log(K_aC_P)
F_0

Figure 4

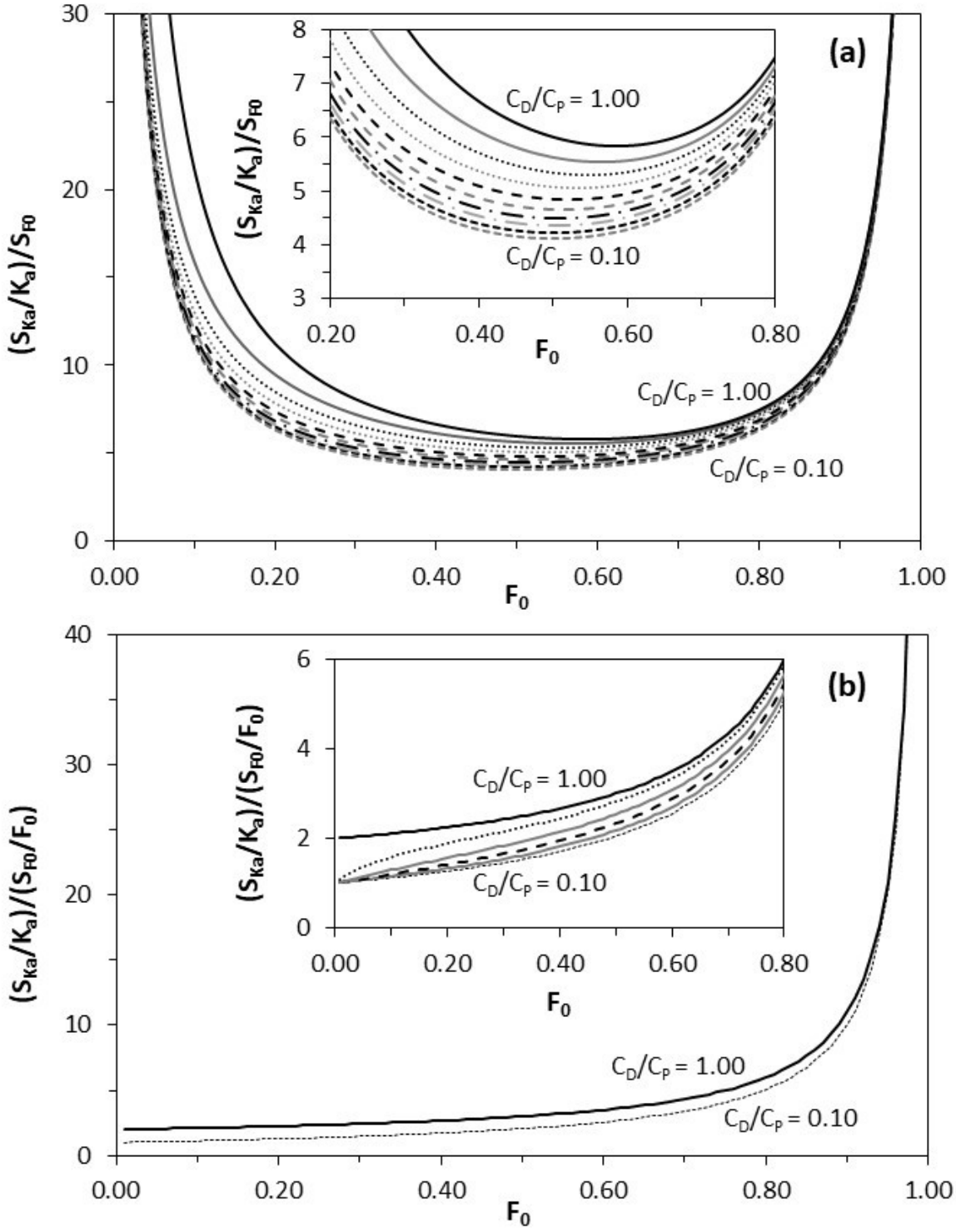
(a)
$(S_{Ka}/K_a)/S_{F0}$
F_0
C_D/C_P = 1.00
C_D/C_P = 0.10
(b)
$(S_{Ka}/K_a)/(S_{F0}/F_0)$
F_0
C_D/C_P = 1.00
C_D/C_P = 0.10

Figure 5

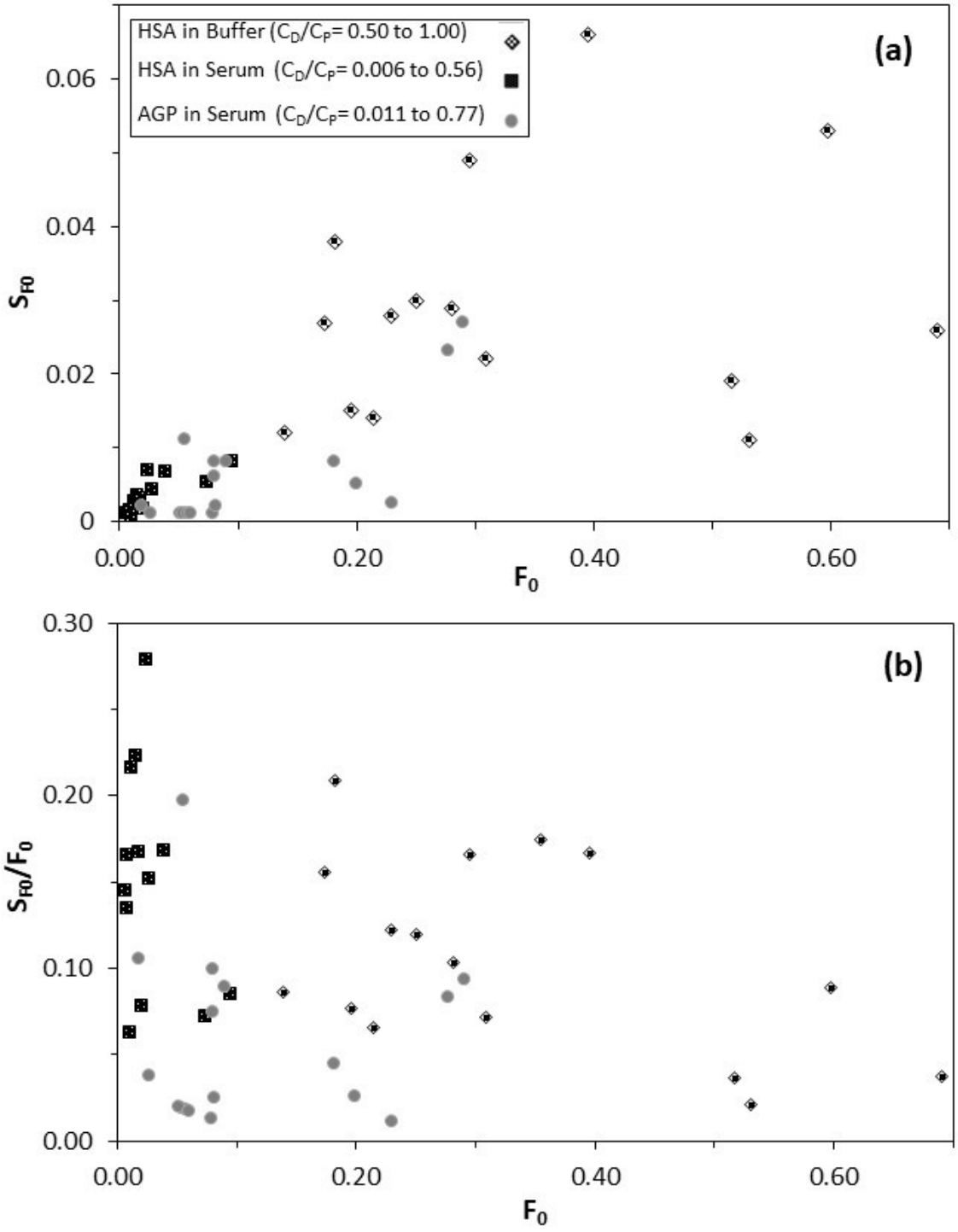
HSA in Buffer (C_D/C_P= 0.50 to 1.00)
HSA in Serum (C_D/C_P= 0.006 to 0.56)
AGP in Serum (C_D/C_P= 0.011 to 0.77)
(a)
S_{F0}
F_0
0.06
0.04
0.02
0
0.00
0.20
0.40
0.60
(b)
S_{F0}/F_0
F_0
0.30
0.20
0.10
0.00
0.00
0.20
0.40
0.60

Figure 6

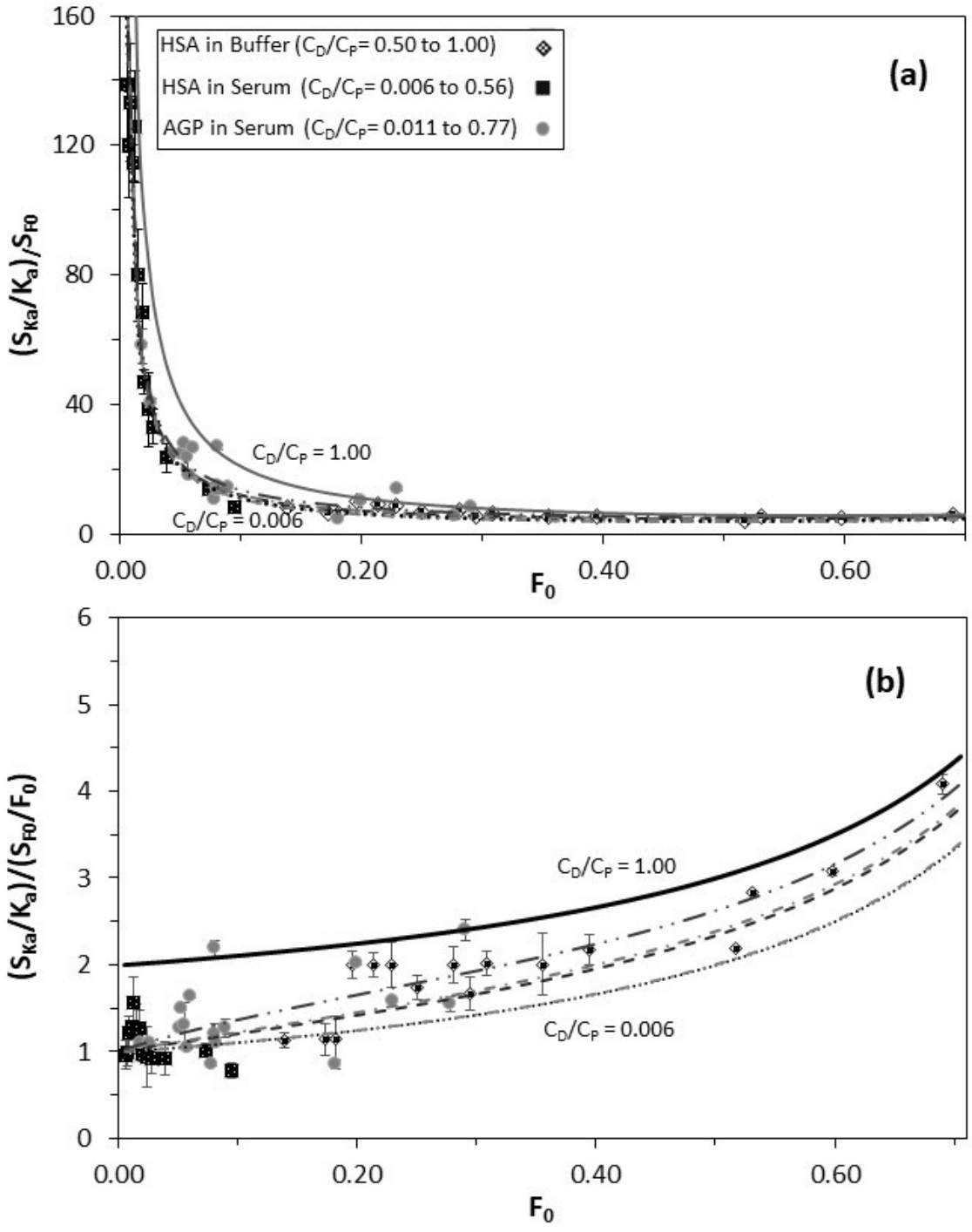
HSA in Buffer (C_D/C_P= 0.50 to 1.00)
HSA in Serum (C_D/C_P= 0.006 to 0.56)
AGP in Serum (C_D/C_P= 0.011 to 0.77)
(a)
$(S_{Ka}/K_a)/S_{F0}$
C_D/C_P = 1.00
C_D/C_P = 0.006
F_0
(b)
$(S_{Ka}/K_a)/(S_{F0}/F_0)$
C_D/C_P = 1.00
C_D/C_P = 0.006
F_0

Figure 7

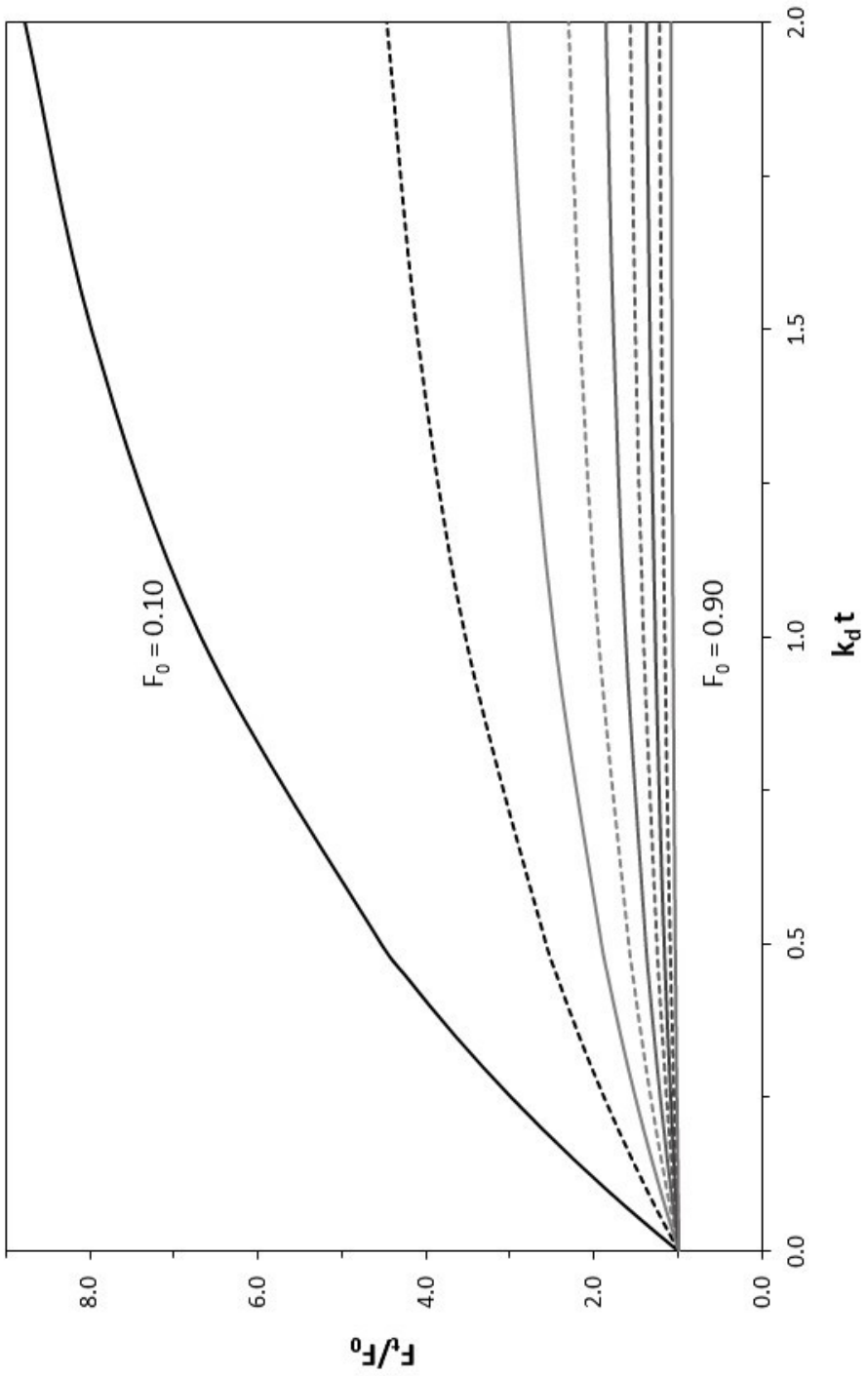

Figure 8

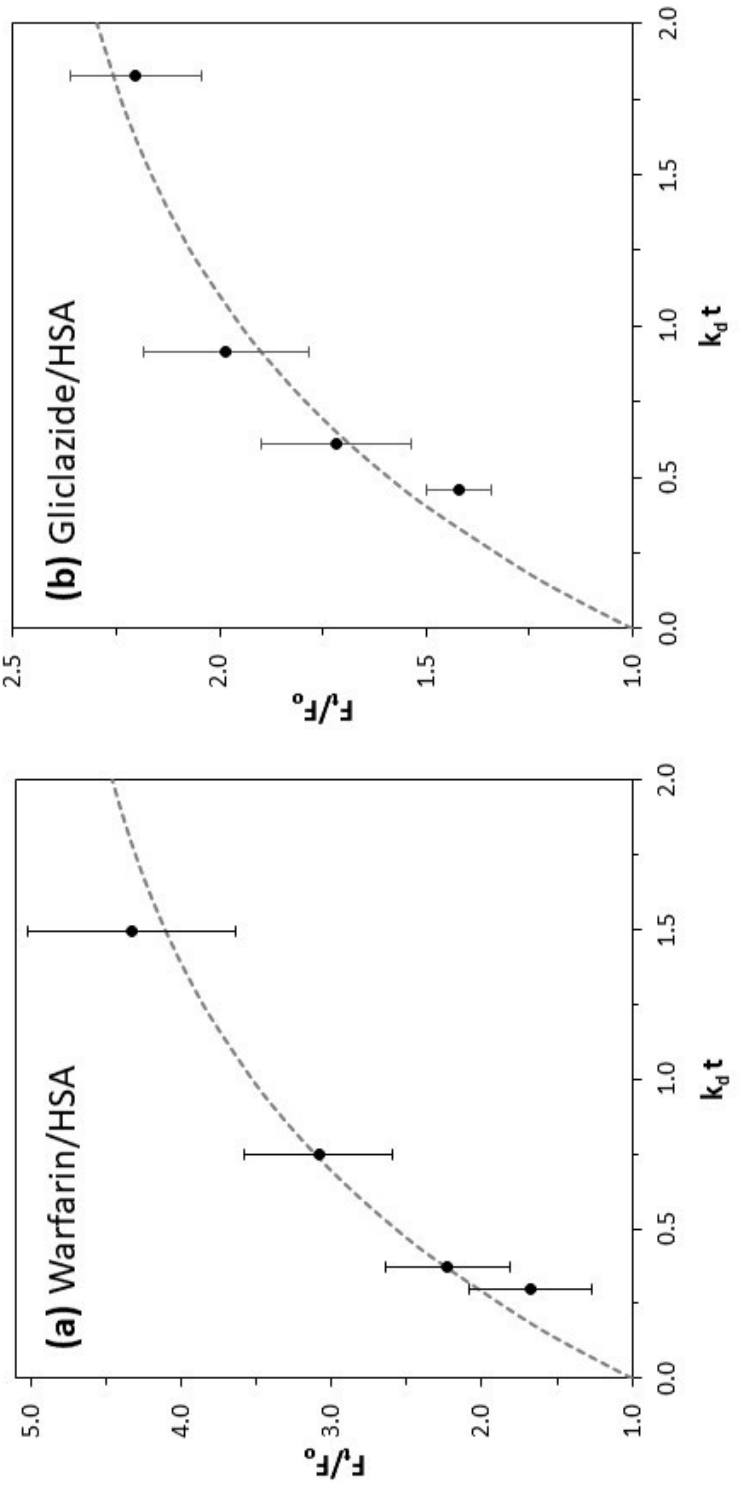
(a) Warfarin/HSA
(b) Gliclazide/HSA
F/F°
k_d t
5.0
4.0
3.0
2.0
1.0
2.5
1.5
0.0
0.5
1.0
1.5
2.0

Figure 9

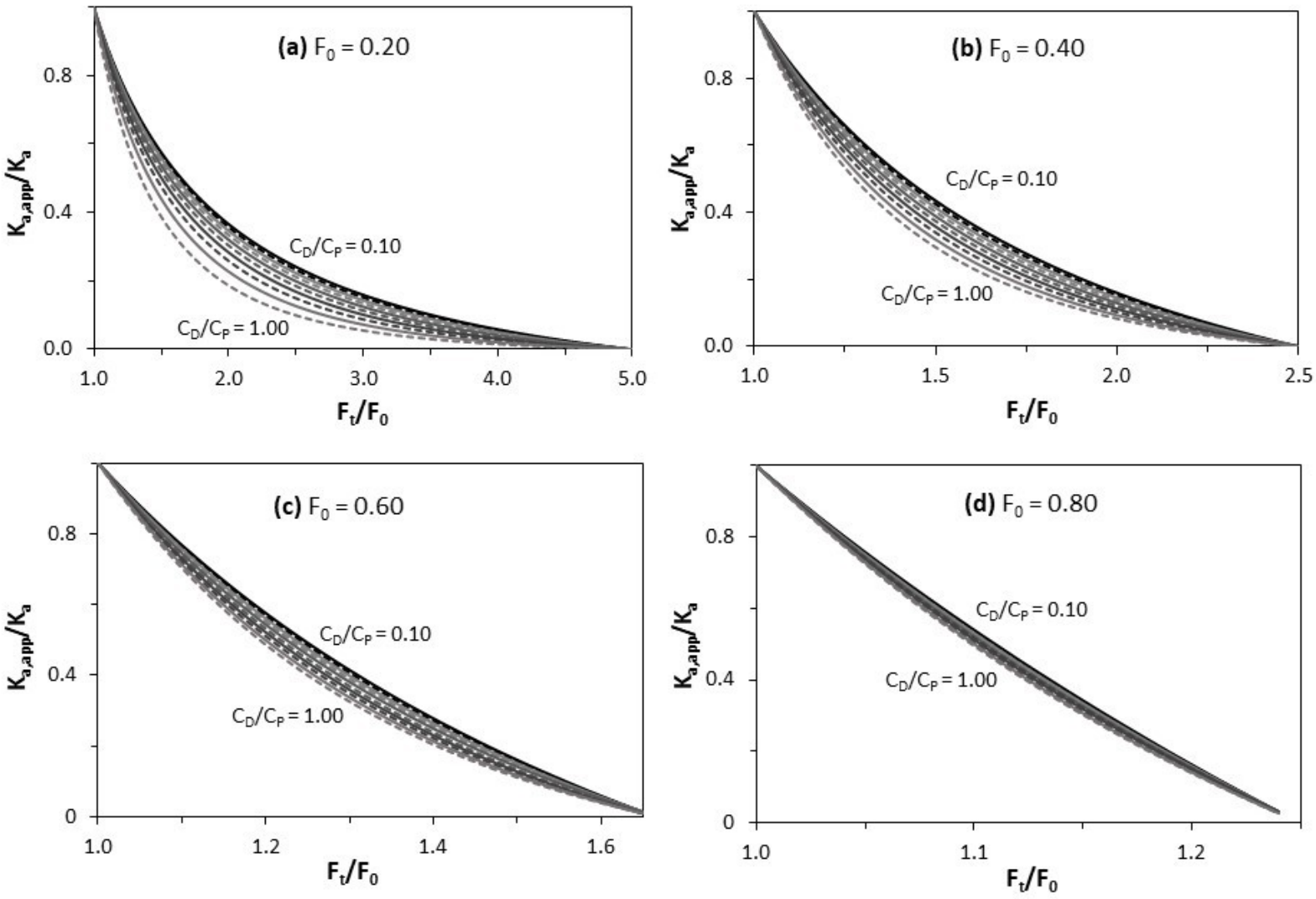

Figure 10

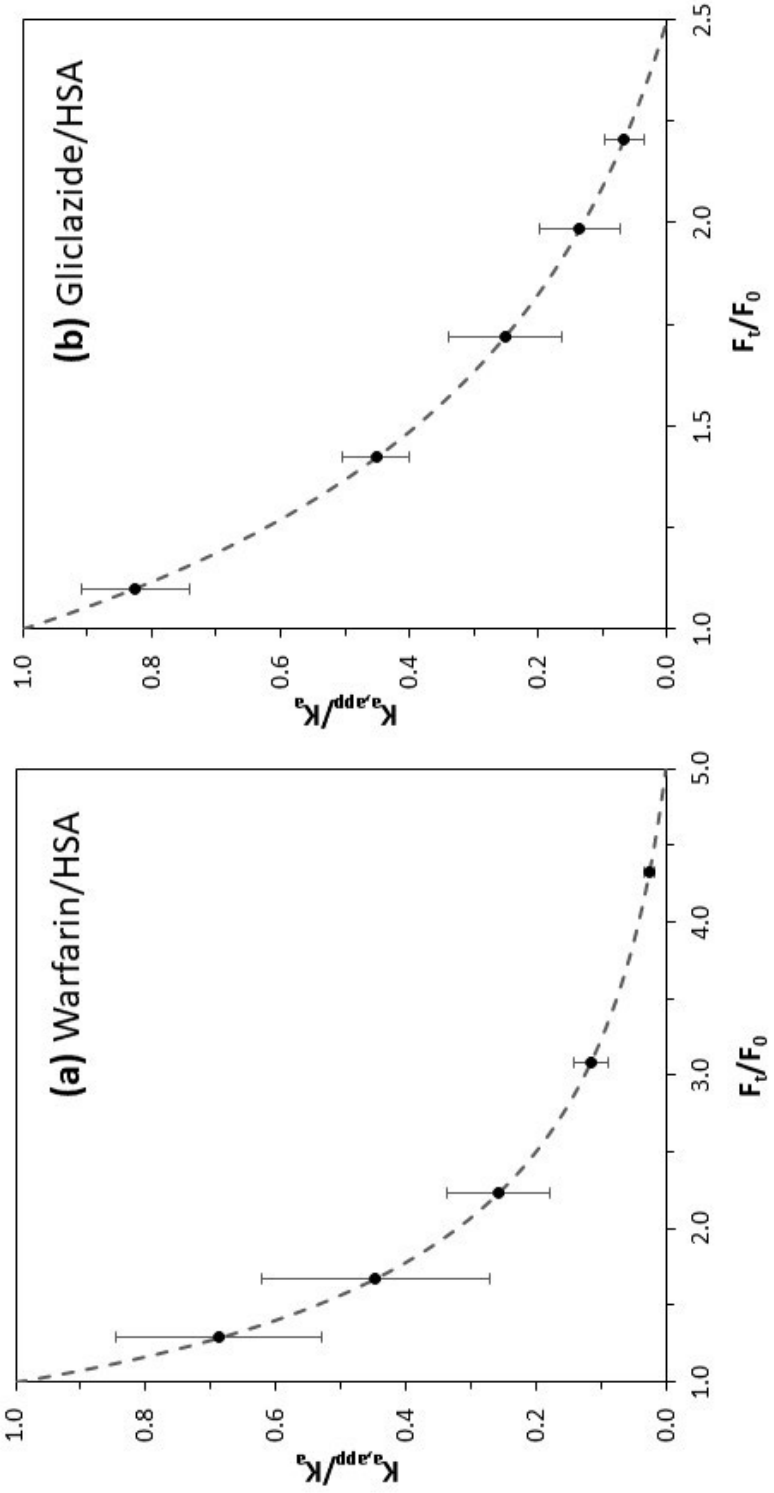
(a) Warfarin/HSA
(b) Gliclazide/HSA
$K_{a,app}/K_a$
F_t/F_0
0.0
0.2
0.4
0.6
0.8
1.0
1.0
2.0
3.0
4.0
5.0
1.5
2.5

Figure 11

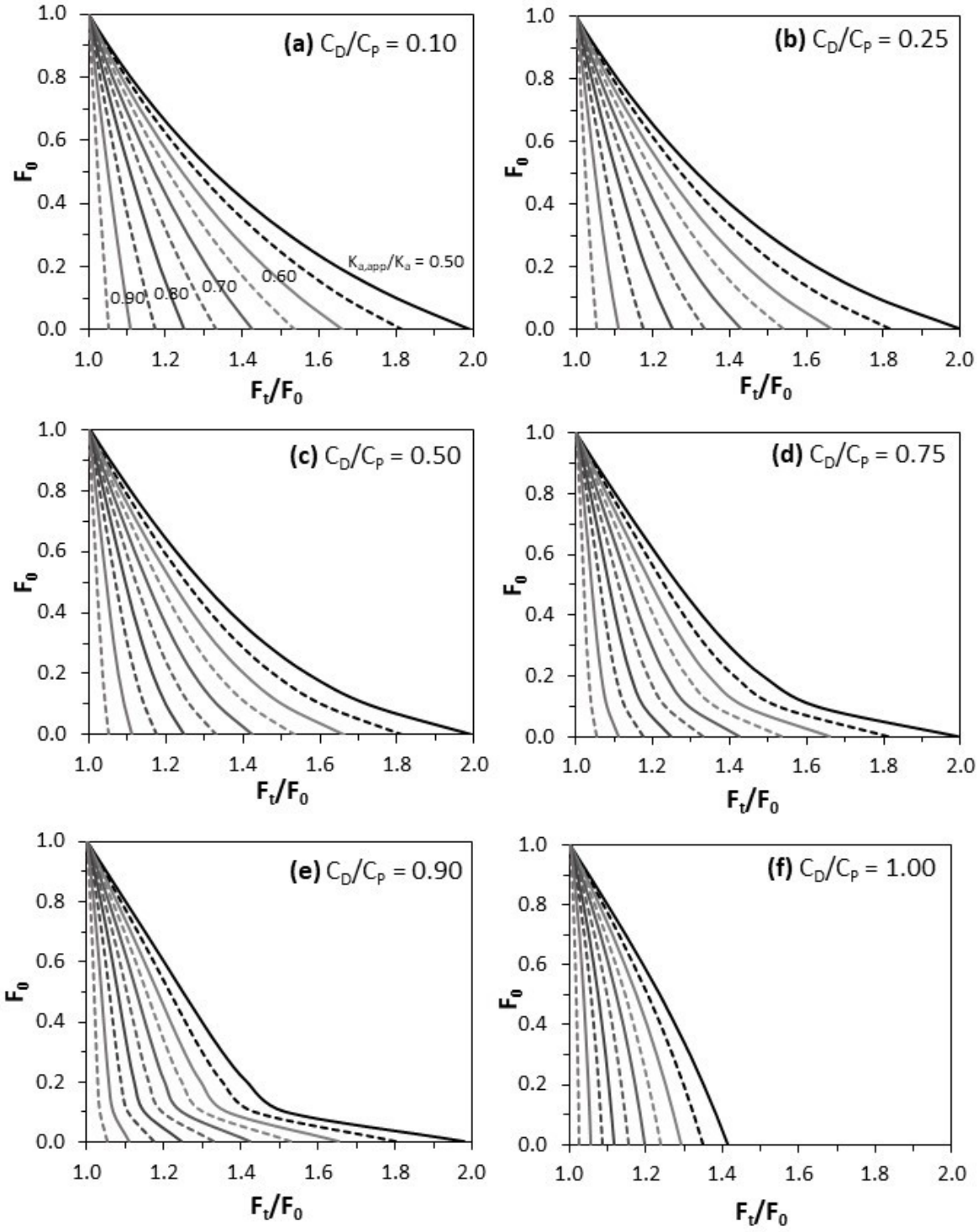
(a) C_D/C_P = 0.10
(b) C_D/C_P = 0.25
(c) C_D/C_P = 0.50
(d) C_D/C_P = 0.75
(e) C_D/C_P = 0.90
(f) C_D/C_P = 1.00
$K_{a,app}/K_a$ = 0.50
0.60
0.70
0.80
0.90
F_0
F_t/F_0
1.0
0.8
0.6
0.4
0.2
0.0
1.0
1.2
1.4
1.6
1.8
2.0

Figure 12

Supplemental Material

Derivation of equation relating free fraction F_0 to the association equilibrium constant K_a

The following reaction describes a system with 1:1 saturable and reversible binding between a solute or drug (D) and a serum protein or binding agent (P) [1,2].

$$D + P \underset{\leftarrow}{\overset{\rightarrow}{}} DP \tag{S1}$$

The association equilibrium constant for this system (K_a) is given by the following relationship [1,2].

$$K_a = \frac{[DP]}{[D][P]} \tag{S2}$$

In this equation, [D] and [P] are the molar concentrations of the solute/drug and protein/binding agent in their non-bound, or free, forms at equilibrium, while [DP] is the molar concentration of the complex formed between D and P. This system can also be described by the following mass balance equations.

$$C_D = [D] + [DP] \quad \text{or} \quad [D] = C_D - [DP] \tag{S3}$$

$$C_P = [P] + [DP] \quad \text{or} \quad [P] = C_P - [DP] \tag{S4}$$

The term C_D in these equations is the total molar concentration for all forms of D in the original mixture containing D and P. In the same manner, the term C_P is the total molar concentration for all forms of the protein/binding agent in this mixture.

The fraction of the non-bound form of D in the original mixture and at equilibrium (F_0) can be obtained from the mass balance expression in eq. (S3).

$$F_0 = \frac{[D]}{[D] + [DP]} = \frac{[D]}{C_D} = \frac{C_D - [DP]}{C_D} = 1 - \frac{[DP]}{C_D} \tag{S5}$$

In addition, the value of [DP] can be found from the values of F_0 and C_D by rearranging eq. (S5), as illustrated in eq. (S6).

$$[DP] = C_D(1 - F_0) \tag{S6}$$

Substituting eqs. (S3) and (S4) into eq. (S2) results in the relationship for K_a that is provided in eq. (S7).

$$K_a = \frac{[DP]}{(C_D - [DP])(C_P - [DP])} \tag{S7}$$

Eq. (S8) is obtained when the terms in the denominator of eq. (S7) are expanded through multiplication.

$$K_a = \frac{[DP]}{C_D C_P - C_D[DP] - C_P[DP] + [DP]^2} \tag{S8}$$

The term [DP] in eq. (S8) can be expressed in terms of F_0 and C_D by using eq. (S6). Combining eqs. (S6) and (S8) results in eq. (S9).

$$K_a = \frac{C_D(1 - F_0)}{C_D C_P - C_D(C_D - C_D F_0) - C_P(C_D - C_D F_0) + (C_D - C_D F_0)^2} \tag{S9}$$

Eq. (S9) can be simplified through multiplication and combination of common terms in the denominator, which produces eq. (S10).

$$K_a = \frac{C_D(1 - F_0)}{{C_D}^2 {F_0}^2 - {C_D}^2 F_0 + C_D C_P F_0} \tag{S10}$$

The expression in eq. (S10) can be further simplified by factoring out the term C_D from the numerator and denominator, as shown in eq. (S11).

$$K_a = \frac{C_D(1 - F_0)}{C_D({C_D}{F_0}^2 - C_D F_0 + C_P F_0)} \tag{S11}$$

It is now possible to eliminate one of the terms for C_D from the numerator and denominator by division and to factor F_0 out from all terms in the denominator. This produces the expression for K_a that is given in eq. (S12) in terms of C_D, C_P, and F_0 [3-5].

$$K_a = \frac{(1 - F_0)}{F_0(C_P - C_D + C_D F_0)} \tag{S12}$$

Eq. (S12) can be further simplified by factoring out C_P from all terms in the denominator. The expression for K_a can then be written in terms of F_0, C_P, and the ratio C_D/C_P, as shown in eq. (S13) and given by eq. (1) in the main body of the text.

$$K_a = \frac{(1-F_0)}{F_0 C_P\left(1-\frac{C_D}{C_P}+\frac{C_D}{C_P}F_0\right)} \tag{S13}$$

Effect of systematic errors in the free fraction on a calculated association equilibrium constant

If the measured or apparent free fraction F_t at column residence time t is for a system that is not at equilibrium, the association equilibrium constant that is obtained by using F_t gives an apparent value for the association equilibrium constant between D and P ($K_{a,app}$) that is only an estimate of the true value K_a. The value for $K_{a,app}$ that is obtained based on F_t is given by the modified form of eq. (S13) that is shown in eq. (S14) and eq. (10) in the main body of the text.

$$K_{a,app} = \frac{(1-F_t)}{F_t C_P\left(1-\frac{C_D}{C_P}+\frac{C_D}{C_P}F_t\right)} \tag{S14}$$

Because F_t must be greater than or equal to F_0 in ultrafast affinity extraction (UAE) (i.e., due to possible dissociation of some solute from its binding agent), it would be expected that the value of $K_{a,app}$ will always be less than or equal to K_a. The relative value of $K_{a,app}$ when compared to K_a can be obtained by dividing eq. (S13) by eq. (S14), as shown in eq. (S15).

$$\frac{K_{a,app}}{K_a} = \left[\frac{(1-F_t)}{F_t C_P\left(1-\frac{C_D}{C_P}+\frac{C_D}{C_P}F_t\right)}\right] \Big/ \left[\frac{(1-F_0)}{F_0 C_P\left(1-\frac{C_D}{C_P}+\frac{C_D}{C_P}F_0\right)}\right] \tag{S15}$$

This equation can be further simplified by factoring out F_0/F_t, as illustrated in eq. (S16).

$$\frac{K_{a,app}}{K_a} = \left(\frac{F_0}{F_t}\right)\left[\frac{(1-F_t)}{\left(1-\frac{C_D}{C_P}+\frac{C_D}{C_P}F_t\right)}\right] \Big/ \left[\frac{(1-F_0)}{\left(1-\frac{C_D}{C_P}+\frac{C_D}{C_P}F_0\right)}\right] \tag{S16}$$

In addition, F_t can be replaced with the equivalent term $\{F_0\,(F_t/F_0)\}$ to produce the expression that is shown in eq. (S17) and given as eq. (11) in the main body of the text.

$$\frac{K_{a,app}}{K_a} = \left(\frac{F_0}{F_t}\right)\left[\frac{1-F_0\left(\frac{F_t}{F_0}\right)}{\left(1-\frac{C_D}{C_P}+\frac{C_D}{C_P}F_0\left\{\frac{F_t}{F_0}\right\}\right)}\right] \Big/ \left[\frac{1-F_0}{\left(1-\frac{C_D}{C_P}+\frac{C_D}{C_P}F_0\right)}\right] \qquad \text{(S17)}$$

This final expression was employed in the main body of this paper to generate universal plots to see how the value of $K_{a,app}$ vs K_a changes as a function of F_0, F_t/F_0, and C_D/C_P for a solute and binding agent mixture that is examined by UAE.

Error propagation in relating a measured free fraction to an association equilibrium constant

Eq. (S12), and the equivalent expression in eq. (S13), show how the value of an association equilibrium constant (K_a) can be determined from the original free fraction (F_0) for solute D at equilibrium in a mixture with binding agent P for a system with a 1:1 interaction, and in a situation where the total molar concentrations of D (C_D) and P (C_P) are also known [3–5]. It is reasonable to expect in this type of analysis that the uncertainty in the measured value of F_0 will be much larger than the uncertainties in C_D and C_P (i.e., due the high precisions in mass and volume measurements that are often used to prepare samples or reagents for analysis) [6]. If this is the case, then the uncertainty in K_a, as represented by its standard deviation (S_{K_a}), can be estimated from the uncertainty in F_0 by using error propagation.

The first step in this error propagation involves taking the derivative of K_a with respect to F_0 in eq. (S12), with the values of C_D and C_P being treated as constants. The general formula for error propagation that relates S_{K_a} to the standard deviation of F_0 (S_{F_0}) is shown in eq. (S18) [6].

$$\left(S_{K_a}\right)^2 \approx \left(\frac{\delta_{K_a}}{\delta_{F_0}}\right)^2 \left(S_{F_0}\right)^2 \qquad \text{or} \qquad S_{K_a} \approx \sqrt{\left(\frac{\delta_{K_a}}{\delta_{F_0}}\right)^2 \left(S_{F_0}\right)^2} \qquad \text{(S18)}$$

In this equation, $\frac{\delta_{K_a}}{\delta_{F_0}}$ is the derivative of K_a with respect to F_0 in eq. (S12). When this derivative is found, the following result is obtained.

$$\frac{\delta_{K_a}}{\delta_{F_0}} = \frac{(-F_0)(C_P - C_D + C_D F_0) - (1-F_0)(C_P - C_D + C_D(2F_0))}{(F_0(C_P - C_D + C_D F_0))^2} \quad \text{(S19)}$$

Factoring out C_P from the numerator and denominator of eq. (S19) gives the expression shown in eq. (S20).

$$\frac{\delta_{K_a}}{\delta_{F_0}} = \frac{(-F_0)(C_P)\left(1 - \frac{C_D}{C_P} + \frac{C_D}{C_P}F_0\right) - (1-F_0)(C_P)\left(1 - \frac{C_D}{C_P} + \frac{C_D}{C_P}(2F_0)\right)}{{C_P}^2\left(F_0\left(1 - \frac{C_D}{C_P} + \frac{C_D}{C_P}F_0\right)\right)^2} \quad \text{(S20)}$$

Eq. (S20) can be further expanded into the form provided in eq. (S21).

$$\frac{\delta_{K_a}}{\delta_{F_0}} = \frac{(-F_0)(C_P)\left(1 - \frac{C_D}{C_P} + \frac{C_D}{C_P}F_0\right) - (1-F_0)(C_P)\left(1 - \frac{C_D}{C_P} + \frac{C_D}{C_P}(F_0)\right) - (1-F_0)(C_P)\left(\frac{C_D}{C_P}(F_0)\right)}{{C_P}^2\left(F_0\left(1 - \frac{C_D}{C_P} + \frac{C_D}{C_P}F_0\right)\right)^2} \quad \text{(S21)}$$

Eq. (S21) can be simplified by cancelling out one of the terms for C_P that appears in both the numerator and denominator of eq. (S21). This simplification gives the expression for $\frac{\delta_{K_a}}{\delta_{F_0}}$ that is shown in eq. (S22).

$$\frac{\delta_{K_a}}{\delta_{F_0}} = \frac{(-F_0)\left(1 - \frac{C_D}{C_P} + \frac{C_D}{C_P}F_0\right) - (1-F_0)\left(1 - \frac{C_D}{C_P} + \frac{C_D}{C_P}(F_0)\right) - (1-F_0)\left(\frac{C_D}{C_P}(F_0)\right)}{C_P\left(F_0\left(1 - \frac{C_D}{C_P} + \frac{C_D}{C_P}F_0\right)\right)^2} \quad \text{(S22)}$$

It is possible to modify eq. (S22) by dividing the left and right sides of this expression with the ratio of the right and left terms in eq. (S13). This modification results in eq. (S23).

$$\frac{\delta_{K_a}}{\delta_{F_0}} = (K_a)\frac{(-F_0)\left(1 - \frac{C_D}{C_P} + \frac{C_D}{C_P}F_0\right) - (1-F_0)\left(1 - \frac{C_D}{C_P} + \frac{C_D}{C_P}(F_0)\right) - (1-F_0)\left(\frac{C_D}{C_P}(F_0)\right)}{F_0(1-F_0)\left(\left(1 - \frac{C_D}{C_P} + \frac{C_D}{C_P}F_0\right)\right)} \quad \text{(S23)}$$

Eq. (S23) can be further simplified by dividing the numerator on the right side of this expression by the denominator. This change makes it possible to express $\frac{\delta_{K_a}}{\delta_{F_0}}$ as shown in eq. (S24).

$$\frac{\delta_{K_a}}{\delta_{F_0}} = (-K_a)\left(\frac{1}{(1-F_0)} + \frac{1}{F_0} + \frac{\left(\frac{C_D}{C_P}\right)}{\left(1 - \frac{C_D}{C_P} + \frac{C_D}{C_P}F_0\right)}\right) \quad \text{(S24)}$$

The following expression for S_{K_a} is obtained by substituting eq. (S24) into eq. (S18).

$$S_{K_a} \approx \sqrt{\left((-K_a)\left(\frac{1}{(1-F_0)} + \frac{1}{F_0} + \frac{\left(\frac{C_D}{C_P}\right)}{\left(1-\frac{C_D}{C_P}+\frac{C_D}{C_P}F_0\right)}\right)\right)^2 (S_{F_0})^2} \quad \text{(S25)}$$

Eq. (S25) can be further revised by dividing both sides of this expression by K_a and simplifying the combined squared/square root term on the right. These modifications result in the relationship that is shown in eq. (S26). This is the same expression that is given as eq. (4) in the main body of the text.

$$\frac{S_{K_a}}{K_a} \approx (S_{F_0})\left(\frac{1}{(1-F_0)} + \frac{1}{F_0} + \frac{\left(\frac{C_D}{C_P}\right)}{\left(1-\frac{C_D}{C_P}+\frac{C_D}{C_P}F_0\right)}\right) \quad \text{(S26)}$$

Multiplying the right side of eq. (S26) by F_0/F_0 (i.e., a term equal to one) results in the following expression that relates the relative precision of K_a to the relative precision of F_0; this is the same relationship that is given as eq. (5) in the main body of the text.

$$\frac{S_{K_a}}{K_a} \approx \left(\frac{S_{F_0}}{F_0}\right)\left(\frac{F_0}{(1-F_0)} + 1 + \frac{F_0\left(\frac{C_D}{C_P}\right)}{\left(1-\frac{C_D}{C_P}+\frac{C_D}{C_P}F_0\right)}\right) \quad \text{(S27)}$$

Eqs. (S26) and (S27) both show how the relative precision of K_a, as represented by the ratio (S_{K_a}/K_a), is related to unitless values such as the absolute or relative precision of F_0 (as described by S_{F_0} or S_{F_0}/F_0, respectively), the value of F_0, and the ratio of the total molar concentrations for D and P (i.e., C_D/C_P).

General error propagation formula for the precision of an association equilibrium constant

The same approach as used in the previous section can be used to obtain a more general expression for error propagation that considers how the uncertainties in both F_0 and the total molar

concentrations for D and P affect the uncertainty in K_a for a system with a 1:1 interaction between D and P. To do this, the expanded error propagation formulas that are shown below in eq. (S28) can be written to include the standard deviations for C_D and C_P and the derivatives for K_a with respect to each of these terms [6].

$$\left(S_{K_a}\right)^2 = \left(\frac{\delta K_a}{\delta F_0}\right)^2 \left(S_{F_0}\right)^2 + \left(\frac{\delta K_a}{\delta C_D}\right)^2 \left(S_{C_D}\right)^2 + \left(\frac{\delta K_a}{\delta C_P}\right)^2 \left(S_{C_P}\right)^2$$

$$\text{or} \qquad S_{K_a} = \sqrt{\left(\frac{\delta K_a}{\delta F_0}\right)^2 \left(S_{F_0}\right)^2 + \left(\frac{\delta K_a}{\delta C_D}\right)^2 \left(S_{C_D}\right)^2 + \left(\frac{\delta K_a}{\delta C_P}\right)^2 \left(S_{C_P}\right)^2} \tag{S28}$$

The terms $\frac{\delta K_a}{\delta C_D}$ and $\frac{\delta K_a}{\delta C_P}$ in this equation are found by taking the derivative of K_a in eq. (S12) with respect to C_D or C_P, respectively.

$$\frac{\delta K_a}{\delta C_D} = \frac{(1-F_0)^2}{F_0(C_P - C_D + C_D F_0)^2} \tag{S29}$$

$$\frac{\delta K_a}{\delta C_P} = \frac{-(1-F_0)}{F_0(C_P - C_D + C_D F_0)^2} \tag{S30}$$

Alternative expressions for eqs. (S29) and (S30) can be obtained by dividing the left and right sides of these relationships by left and right terms of eq. (S12) and rearranging into the forms given in eqs. (S31-S32).

$$\frac{\delta K_a}{\delta C_D} = (K_a)\left(\frac{(1-F_0)}{(C_P - C_D + C_D F_0)}\right) \tag{S31}$$

$$\frac{\delta K_a}{\delta C_P} = (K_a)\left(\frac{-1}{(C_P - C_D + C_D F_0)}\right) \tag{S32}$$

The following expanded expression for S_{K_a} with respect to the combined uncertainties in F_0, C_D, and C_P is obtained by substituting eqs. (S24), (S31), and (S32) into eq. (S28).

$$\left(S_{K_a}\right)^2 = \left((-K_a)\left(\frac{1}{(1-F_0)} + \frac{1}{F_0} + \frac{\left(\frac{C_D}{C_P}\right)}{\left(1-\frac{C_D}{C_P}+\frac{C_D}{C_P}F_0\right)}\right)\right)^2 \left(S_{F_0}\right)^2 + \left((K_a)\left(\frac{(1-F_0)}{(C_P-C_D+C_DF_0)}\right)\right)^2 \left(S_{C_D}\right)^2 + \left((K_a)\left(\frac{-1}{(C_P-C_D+C_DF_0)}\right)\right)^2 \left(S_{C_P}\right)^2 \quad \text{(S33)}$$

An expression can also be obtained for the relative precision of K_a, as represented by the ratio (S_{K_a}/K_a), in terms of the absolute precisions for F_0, C_D, and C_P by dividing both the left and right sides of eq. (S33) by $(K_a)^2$.

$$\left(S_{K_a}/K_a\right)^2 = \left(\frac{1}{(1-F_0)} + \frac{1}{F_0} + \frac{\left(\frac{C_D}{C_P}\right)}{\left(1-\frac{C_D}{C_P}+\frac{C_D}{C_P}F_0\right)}\right)^2 \left(S_{F_0}\right)^2 + \left(\frac{(1-F_0)}{(C_P-C_D+C_DF_0)}\right)^2 \left(S_{C_D}\right)^2 + \left(\frac{-1}{(C_P-C_D+C_DF_0)}\right)^2 \left(S_{C_P}\right)^2 \quad \text{(S34)}$$

Finally, a related expression in terms of the relative precisions of F_0, C_D, and C_P can be derived from eq. (S34) by multiplying the individual terms on the right for these variables by $(F_0/F_0)^2$, $(C_D/C_D)^2$, and $(C_P/C_P)^2$, respectively, and rearranging into eq. (S35).

$$\left(S_{K_a}/K_a\right)^2 = \left(\frac{F_0}{(1-F_0)} + 1 + \frac{F_0\left(\frac{C_D}{C_P}\right)}{\left(1-\frac{C_D}{C_P}+\frac{C_D}{C_P}F_0\right)}\right)^2 \left(S_{F_0}/F_0\right)^2 + \left(\frac{(1-F_0)}{(C_P/C_D-1+F_0)}\right)^2 \left(S_{C_D}/C_D\right)^2 + \left(\frac{-1}{\left(1-\frac{C_D}{C_P}+\frac{C_D}{C_P}F_0\right)}\right)^2 \left(S_{C_P}/C_P\right)^2 \quad \text{(S35)}$$

In eq. (S35), the relative precision of K_a, or (S_{K_a}/K_a), is related to the relative precisions of F_0, C_D, and C_P and to dimensionless values such as F_0 and the ratio of the total molar concentrations for D and P (i.e., C_D/C_P).

Figure 1S was generated by using eq. (S35) to show how relative precisions of F_0, C_D, and C_P each contribute to the relative precision of K_a. In this plot, the three lines that are shown for $\left(\frac{\delta_{K_a}}{\delta_{F_0}}\right)^2_{\text{Rel}}$, $\left(\frac{\delta_{K_a}}{\delta_{C_D}}\right)^2_{\text{Rel}}$, and $\left(\frac{\delta_{K_a}}{\delta_{C_P}}\right)^2_{\text{Rel}}$ represent the calculated values of the squares for the combined derivatives and relative standard deviation terms on the right side of eq. (S35) for F_0, C_D, and C_P.

In addition, the relative standard deviation for each of these terms was set equal to a value of 1.00 in this plot to allow the behaviors of the derivative portions for these terms to be directly compared. A C_D/C_P ratio of 1.00 was also used in this comparison (Note: This represents the conditions in which the C_D and C_P terms have the largest contributions to the uncertainty of K_a, as much smaller contributions are seen in similar plots prepared at lower C_D/C_P ratios).

It can be seen from Figure 1S that the contribution to the relative precision of K_a by the relative precision in F_0 is largest as the value of F_0 grows over 0.80 and approaches 1.00. This is the same result that is obtained with eq. (S27) when the relative precision of F_0 is assumed to be the only significant contribution to the relative precision of K_a. However, Figure 1S also indicates that the relative precisions of C_D and C_P may become important in affecting the relative precision of K_a at low values for F_0 (e.g., 0.20 or less) when the relative standard deviations for C_D and C_P are similar to the relative standard deviation for F_0.

It is further possible to use eq. (S35) to determine which experimental conditions will require that contributions due to the precisions of C_D and C_P be considered with regard to the relative precision of K_a. This can be done by placing into eq. (S35) the values of C_D, C_P, and F_0 that may be present during a binding study, along with estimates of the relative standard deviations for C_D, C_P, and F_0. Examples for such comparisons are provided in Figure 2S, as obtained at a C_D/C_P ratio of 1.00. In these examples, the relative standard deviation for F_0 was set at ± 1% or ± 5%, which represent the highest precisions that have been obtained for this parameter by UAE in binding studies for various drug-protein systems (see summary in Tables 1S-3S) [4,7-11]. The relative standard deviation that was used for both C_D and C_P in Figure 2S was ± 0.1% (i.e., a low-to-moderate estimate of precision for the types of samples and reagents that were employed with UAE for the systems in Tables 1S-3S).

For the situation in Figure 2S(a) and where F_0 had a high relative precision of ± 1%, the relative precision for F_0 made up more than 92.5% of the total contributions to the relative precision of K_a at an F_0 value of 0.20 or greater. In addition, the relative precision of F_0 made up 99.5% of the total contributions to the relative precision of K_a when F_0 was equal to 0.50. When the relative precision of F_0 was set to ± 5%, as illustrated in Figure 2S(b), the relative precision of F_0 made up more than 99.7% of the total contributions to the relative precision K_a at an F_0 value of 0.20 or greater, and 99.98% of the total contributions at $F_0 = 0.50$. It was found that these contributions due to the relative precision of F_0 became even closer to 100% if the relative precision of F_0 became larger (e.g., ± 10-25%, as occurs for some of the experimental systems in Tables 1S-3S), the ratio for C_D/C_P was decreased below 1.00, or the relative precisions for C_D and C_P had values smaller than ± 0.1%.

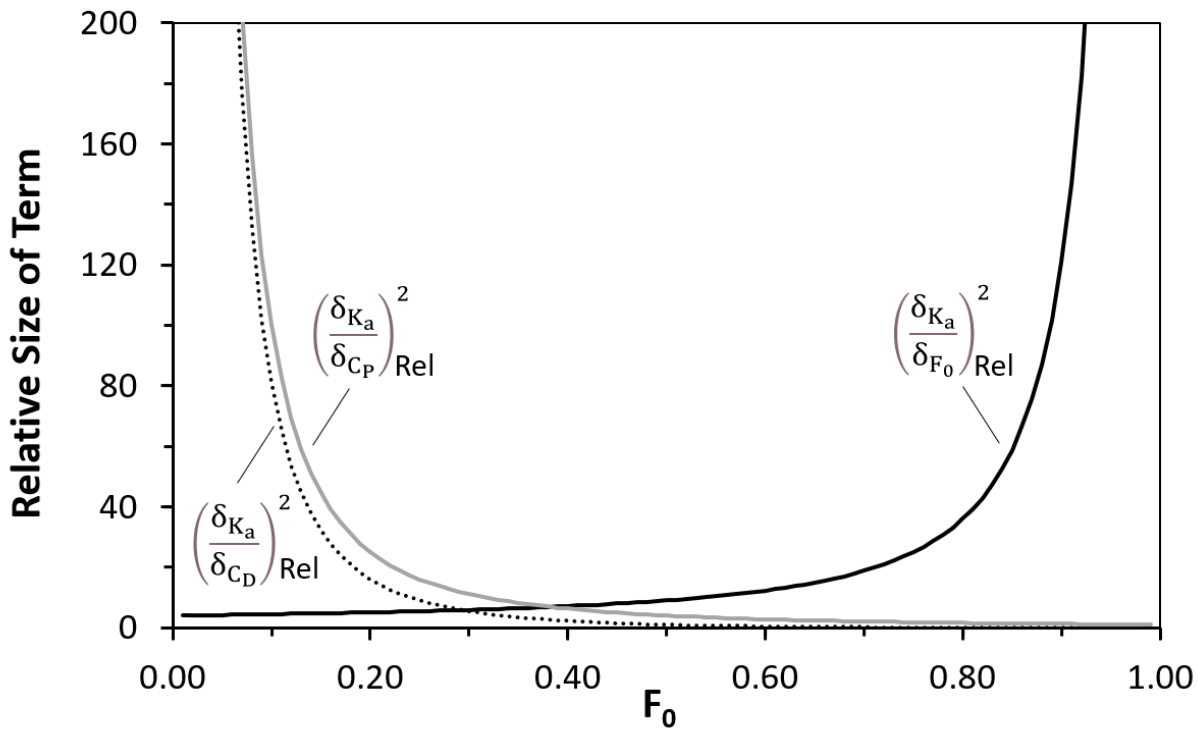

Figure 1S. Illustration of the contributions by the relative precisions of F_0, C_D, and C_P to the relative precision of K_a at $C_D/C_P = 1.00$, as determined by using eq. (S35). The lines shown for $\left(\frac{\delta_{K_a}}{\delta_{F_0}}\right)^2_{Rel}$, $\left(\frac{\delta_{K_a}}{\delta_{C_D}}\right)^2_{Rel}$, and $\left(\frac{\delta_{K_a}}{\delta_{C_P}}\right)^2_{Rel}$ represent the calculated values of the squares for the combined derivatives and relative standard deviation terms on the right side of eq. (S35) for F_0, C_D, and C_P, respectively, with the relative standard deviation for each of these terms being set to unity (i.e., a value of 1.00).

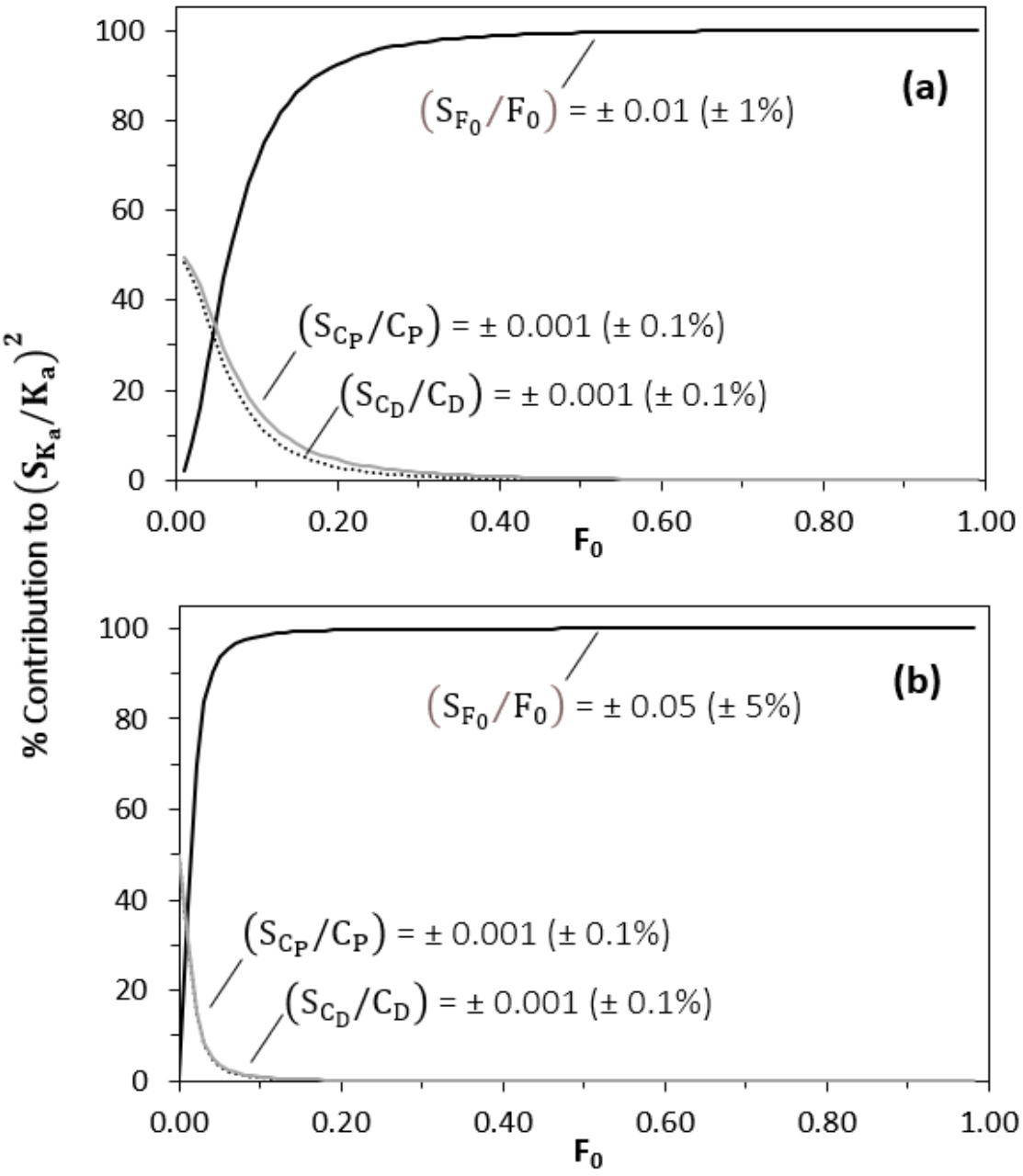

Figure 2S. Estimated overall contributions by the relative precisions of F_0, C_D, and C_P to the relative precision of K_a at $C_D/C_P = 1.00$, as determined by using eq. (S35). The three lines show the contributions expected when the relative standard deviation for F_0 is (a) ± 1% or (b) ± 5% and the relative standard deviations for both C_D and C_P are ± 0.1%.

Results from prior studies using UAE for the determination of association equilibrium constants

Figures 3 and 4 in the main body of the text were created using results and conditions reported in prior studies that employed UAE to estimate the binding constants for various drugs with the serum transport proteins [4,7-11]. These data and conditions are summarized in Tables 1S-3S. Experimental data from the same prior studies [4,7-11] were also used in Figures 6 and 7 to examine how the relative precision of estimates for K_a varied with the conditions used in UAE and precision observed for F_0.

Figure 3 was generated using the data and conditions provided in Table 1S. These data were generated by UAE when using well-controlled mixtures of drug-protein combinations in buffered solutions based on HSA or modified forms of this protein, along with a value for C_D/C_P of 0.50 or 1.00 [4,7,8]. The plots in Figure 4 were prepared in a similar manner by using data and conditions from previous UAE measurements of the free fractions and binding constants of solutes in serum samples, and for which the values of C_P and C_D/C_P were determined by the content of these samples. These results and conditions are listed in Tables 2S-3S and were obtained by UAE for a variety of drugs at typical therapeutic concentrations in serum and with HSA or AGP at normal or disease state concentrations [9-11].

Table 1S. F_0, C_D/C_P, and K_a values for various drugs combined with normal or modified human serum albumin in buffered mixtures examined using UAE[a]

Drug & Protein[b]	C_D/C_P	F_0	K_a (M^{-1})[c]	log(K_a C_P)[c]	Reference
Warfarin-HSA	0.50	0.25 (± 0.03)	2.4 (± 0.5) × 10^5	0.68	[7]
Tolbutamide-HSA	1.00	0.598 (± 0.053)	1.1 (± 0.3) × 10^5	0.05	[4]
Tolbutamide-HSA	0.50	0.395 (± 0.066)	1.1 (± 0.4) × 10^5	0.34	[4]
Acetohexamide-HSA	1.00	0.531 (± 0.011)	1.7 (± 0.1) × 10^5	0.22	[4]
Acetohexamide-HSA	0.50	0.295 (± 0.049)	1.8 (± 0.5) × 10^5	0.57	[4]
Chlorpromazine-HSA	1.00	0.690 (± 0.026)	6.5 (± 1.0) × 10^4	-0.19	[4]
Chlorpromazine-HSA	0.50	0.517 (± 0.019)	6.2 (± 0.5) × 10^4	0.09	[4]
Glibenclamide-HSA	1.00	0.196 (± 0.015)	2.09 (± 0.32) × 10^6	1.32	[8]
Glibenclamide-GHSA1	1.00	0.214 (± 0.014)	1.72 (± 0.23) × 10^6	1.23	[8]
Glibenclamide-GHSA2	1.00	0.229 (± 0.028)	1.47 (± 0.36) × 10^6	1.17	[8]
Glimepiride-HSA	1.00	0.281 (± 0.029)	9.1 (± 1.9) × 10^5	0.96	[8]
Glimepiride-GHSA1	1.00	0.309 (± 0.022)	7.2 (± 1.0) × 10^5	0.86	[8]
Glimepiride-GHSA2	1.00	0.355 (± 0.062)	5.1 (± 1.8) × 10^5	0.71	[8]
Glipizide-HSA	0.50	0.139 (± 0.012)	5.4 (± 0.5) × 10^5	1.04	[8]
Glipizide-GHSA1	0.50	0.173 (± 0.027)	4.1 (± 0.7) × 10^5	0.91	[8]
Glipizide-GHSA2	0.50	0.182 (± 0.038)	3.8 (± 0.9) × 10^5	0.88	[8]

[a]The numbers in the parentheses represent a range of ± 1 S.D. for 3-5 sample injections. These results were acquired at pH 7.4 and 37 (± 0.1) ℃ [4,7,8]. The standard deviations that are provided for K_a were determined through error propagation by using eq. (S25).

[b]Terms: HSA, normal human serum albumin [4,7]; GHSA1, glycated HSA with 15 mM D-glucose; GHSA2, glycated HSA modified with 30 mM D-glucose [8].

[c]For drugs that may have multisite interactions with the given binding agents, the global affinity constant (nK′$_a$) can be used in place of K_a in this table [5].

Table 2S. F_0, C_D/C_P, and K_a values for various drug-HSA interactions analyzed in serum using UAE[a]

Drug & Protein[b]	**C_D/C_P**	**F_0**	**K_a (M^{-1})**[c]	**log(K_a C_p)**[c]	**Reference**
Quinidine-HSA in normal serum	0.016	0.074 (± 0.005)	2.0 (± 0.2) × 10^4	1.10	[9]
Diazepam-HSA in normal serum	0.006	0.0069 (± 0.0010)	2.4 (± 0.3) × 10^5	2.16	[9]
Tolbutamide-HSA in normal serum	0.44	0.0244 (± 0.0068)	1.2 (± 0.3) × 10^5	1.84	[9]
Acetohexamide-HSA in normal serum	0.22	0.0112 (± 0.0007)	1.4 (± 0.1) × 10^5	2.05	[9]
Gliclazide-HSA in normal serum	0.04	0.0206 (± 0.0016)	8.10 (± 0.06) × 10^5	1.69	[9]
Quinidine-HSA in normal serum	0.02	0.0951 (± 0.0080)	2.50 (± 0.02) × 10^5	0.99	[9]
Diazepam-HSA in normal serum	0.01	0.0082 (± 0.0011)	2.5 (± 0.3) × 10^5	2.09	[9]
Tolbutamide-HSA in normal serum	0.56	0.0394 (± 0.0394)	1.2 (± 0.2) × 10^5	1.72	[9]
Acetohexamide-HSA in normal serum	0.28	0.0157 (± 0.0035)	1.4 (± 0.4) × 10^5	1.94	[9]
Gliclazide-HSA	0.05	0.0277 (± 0.0042)	8.1 (± 1.1) × 10^4	1.57	[9]

in normal serum					
Tolbutamide-HSA in diabetic serum	0.42	0.0186 (± 0.0031)	1.1 (± 0.2) × 10^5	1.95	[9]
Acetohexamide-HSA in diabetic serum	0.21	0.0091 (± 0.0015)	1.7 (± 0.3) × 10^5	2.14	[9]
Gliclazide-HSA in diabetic serum	0.03	0.0125 (± 0.0027)	7.9 (± 2.7) × 10^4	1.91	[9]

[a]The numbers in the parentheses represent a range of ± 1 S.D. for 3-5 sample injections. The analysis was performed at pH 7.4 and 37 (± 0.1) °C [9]. The standard deviations that are provided for K_a were determined through error propagation by using eq. (S25).

[b]Terms: HSA, human serum albumin. The HSA in diabetic serum consisted of pooled serum samples from individuals known to have diabetes [9].

[c]For drugs that may have multisite interactions with the given binding agents, the global affinity constant (nK'_a) can be used in place of K_a in this table [5].

Table 3S. F_0, C_D/C_P, and K_a values for drug-AGP interactions analyzed in serum by UAE[a]

Drug & Protein[b]	C_D/C_P	F_0	K_a (M^{-1})[c]	log(K_a C_P)[c]	Reference
Apridine-AGP in SLE serum	0.16	0.054 (± 0.001)	4.5 (± 0.1) × 10^5	1.32	[10]
Propranolol-AGP in SLE serum	0.01	0.058 (± 0.001)	3.1 (± 0.1) × 10^5	1.21	[10]
Disopyramide-AGP in SLE serum	0.41	0.052 (± 0.001)	6.5 (± 0.2) × 10^5	1.47	[10]
Imatinib-AGP in SLE serum	0.05	0.019 (± 0.002)	1.6 (± 0.2) × 10^6	1.74	[10]
Mepivacaine-AGP in SLE serum	0.38	0.230 (± 0.005)	2.9 (± 0.1) × 10^5	0.68	[10]
Apridine-AGP in SLE serum	0.19	0.061 (± 0.001)	4.3 (± 0.1) × 10^5	1.27	[10]
Propranolol-AGP in SLE serum	0.01	0.082 (± 0.002)	2.8 (± 0.1) × 10^5	1.05	[10]
Disopyramide-AGP in SLE serum	0.41	0.079 (± 0.001)	6.2 (± 0.1) × 10^5	1.27	[10]
Imatinib-AGP in SLE serum	0.06	0.027 (± 0.001)	1.3 (± 0.1) × 10^6	1.58	[10]
Mepivacaine-AGP in SLE serum	0.37	0.182 (± 0.008)	3.1 (± 0.1) × 10^5	0.81	[10]

Carbamazepine-AGP in normal serum	0.77	0.2 (± 0.005)	9.9 (± 1.9) × 10^4	1.02	[11]
Disopyramide-AGP in normal serum	0.75	0.081 (± 0.006)	1.0 (± 0.2) × 10^6	1.56	[11]
Disopyramide-AGP in normal serum	0.38	0.056 (± 0.011)	1.1 (± 0.3) × 10^6	1.42	[11]
Lidocaine-AGP in normal serum	0.75	0.291 (± 0.027)	1.6 (± 0.4) × 10^5	0.72	[11]
Lidocaine-AGP in normal serum	0.38	0.278 (± 0.023)	1.4 (± 0.2) × 10^5	0.56	[11]
Propafenone-AGP in normal serum	0.38	0.09 (± 0.008)	6.6 (± 0.8) × 10^5	1.19	[11]
Propafenone-AGP in normal serum	0.26	0.081 (± 0.008)	6.6 (± 0.8) × 10^5	1.17	[11]

[a]The numbers in the parentheses represent a range of ± 1 S.D. for 3-5 sample injections. These analyses were performed at pH 7.4 and 37 (± 0.1) ℃ [10,11]. The standard deviations that are provided for K_a were determined through error propagation by using eq. (S25).

[b]Terms: AGP, alpha$_1$-acid glycoprotein; SLE, systemic lupus erythematosus.

[c]For drugs that may have multisite interactions with the given binding agents, the global affinity constant (nK'_a) can be used in place of K_a in this table [5].

Effect of solute on measured free fractions in UAE

The model used in this report to describe the effect of solute dissociation on a measured free fraction is based on a solute and binding agent with first-order dissociation kinetics on the time scale of the measurement. This model assumes that all the solute in its original free form is captured immediately by the microcolumn used for UAE and that no reassociation of the solute with its soluble binding agent occurs as the sample passes through the microcolumn [4,5]. If reversible 1:1 binding is present between the solute and binding agent, the total relative amount of the solute can be expressed in terms of its initial free fraction (F_0) and its initial bound fraction (B_0). The sum of these two initial fractions for the solute should be equal to one, as indicated by eqs. (S36) and (S37).

$$1 = F_0 + B_0 \qquad \text{(S36)}$$

$$B_0 = 1 - F_0 \qquad \text{(S37)}$$

For a solute with first-order dissociation from its binding agent, the bound fraction of the solute that remains after a column residence time of t can be represented by the term B_t. The remaining bound fraction can, in turn, be described in terms of B_0, the column residence time t, and the dissociation rate constant for the solute from its soluble binding agent (k_d).

$$B_t = B_0\, e^{-k_d t} \qquad \text{(S38)}$$

The relative amount of a solute that is released by dissociation from its binding agent during passage through a microcolumn can be expressed in terms of the difference between B_0 and B_t at column residence time t.

$$B_0 - B_t = B_0 - B_0\, e^{-k_d t} = B_0\left(1 - e^{-k_d t}\right) \qquad \text{(S39)}$$

The corresponding apparent free fraction, F_t, that is obtained in the presence of this additional amount of non-bound solute can then be found by using eq. (S39) to add the difference between

B_0 and B_t to the original free fraction for the solute, F_0. The resulting expression for F_t is provided in eq. (S40).

$$F_t = F_0 + B_0\left(1 - e^{-k_d t}\right) \quad \text{(S40)}$$

Because the initial bound fraction of solute can also be expressed in terms of initial free fraction, it is possible to combine eq. (S37) with eq. (S40) to obtain eq. (S41), where eq. (S41) is same as eq. (8) in the main text.

$$F_t = F_0 + (1 - F_0)\,(1 - e^{-k_d t}) \quad \text{(S41)}$$

Eq. (S41) can be rearranged into the form shown in eq. (S42) by dividing both sides of eq. (41) by F_0 [4,5]. This is the same relationship that is given as eq. (9) in the main body of the text.

$$\frac{F_t}{F_0} = 1 + \left(\frac{1}{F_0} - 1\right)(1 - e^{-k_d t}) \quad \text{(S42)}$$

Expanded views of plots in Figure 7(a)

Figure 3S shows an expanded view of Figure 7(a) from the main body of the text. These views are provided to more clearly show the fit of the experimental data to the behavior predicted by error propagation and chromatographic theory over either (a) a set of narrow and low F_0 values or (b) a set of broad F_0 values. The conditions and data that were used to generate these plots were the same as described in the main text for Figure 7(a).

Figure 3S. Effect of F_0 on the relative precision of K_a, or (S_{Ka}/K_a), when compared to the absolute precision of F_0, as represented by S_{F0}, for data obtained in prior studies examining the binding of various drug-protein systems. The plots in (a) and (b) are expanded views of Figure 7(a) in the main body of the text. The diamonds represent the results obtained for the binding of drugs to HSA in buffer (i.e., normal or glycated HSA), the squares represent the binding of drugs to HSA in serum (i.e., pooled serum from healthy individuals or diabetic patients), and the circles represent the binding of drugs to AGP in serum (i.e., AGP in pooled normal serum or individual serum samples from individuals with SLE). The error bars represent a range of ± 1 S.D. for 3-5 sample injections. The solid and dashed lines in (a) and (b) represent the results obtained at C_D/C_P ratios (from bottom-to-top) of 0.006, 0.011, 0.50, 0.56, 0.77, and 1.00 (i.e., the range of C_D/C_P ratios estimated to be present in the given set of experiments). These graphs were produced using the data provided in Tables 1S-3S.

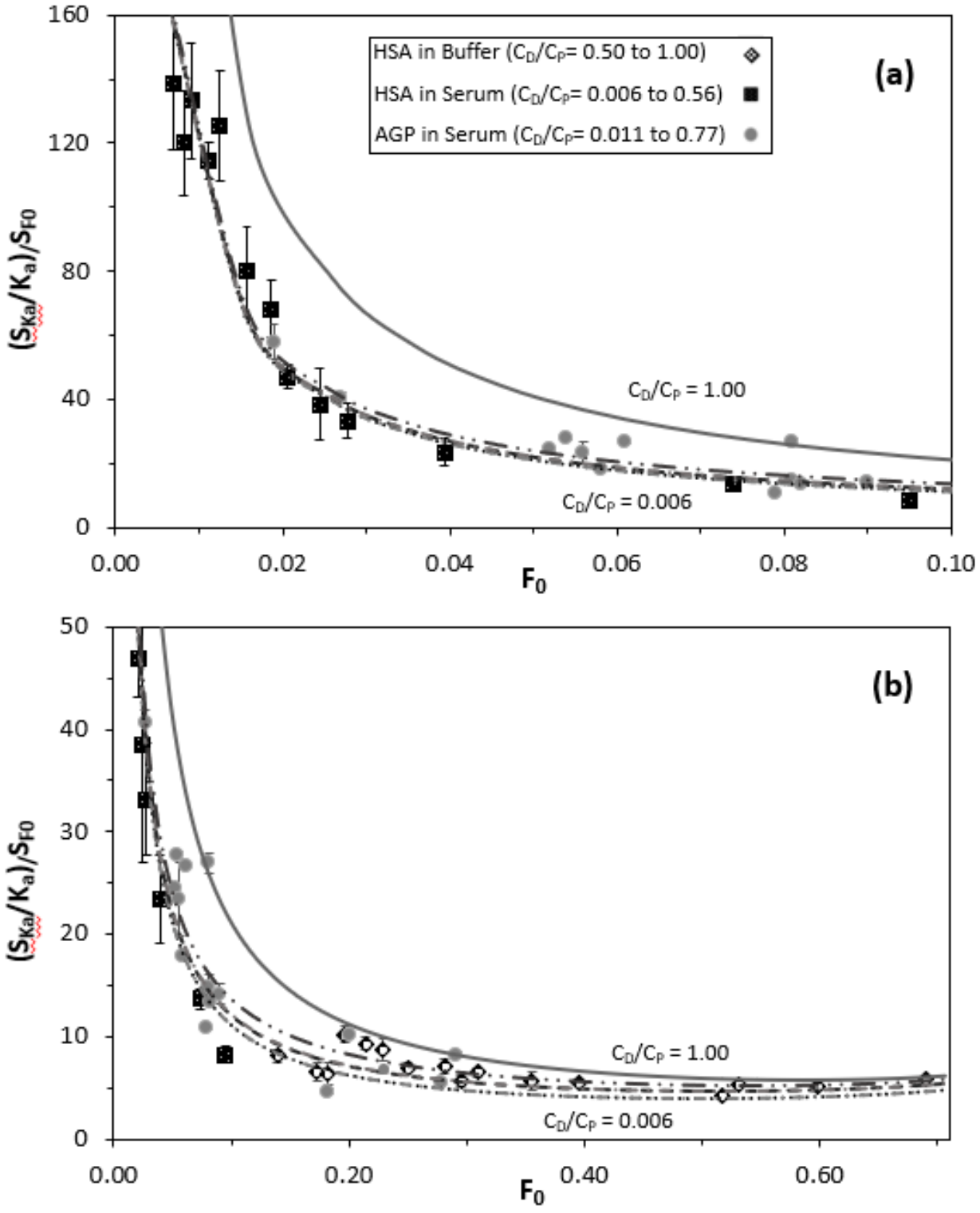
HSA in Buffer (C_D/C_P= 0.50 to 1.00)
HSA in Serum (C_D/C_P= 0.006 to 0.56)
AGP in Serum (C_D/C_P= 0.011 to 0.77)
(a)
C_D/C_P = 1.00
C_D/C_P = 0.006
$(S_{Ka}/K_a)/S_{F0}$
F_0
0
40
80
120
160
0.00
0.02
0.04
0.06
0.08
0.10
(b)
C_D/C_P = 1.00
C_D/C_P = 0.006
$(S_{Ka}/K_a)/S_{F0}$
F_0
0
10
20
30
40
50
0.00
0.20
0.40
0.60

Figure 3S

References

[1] K. Vuignier, J. Schappler, J.-L. Veuthey, P.-A. Carrupt, S. Martel, Drug–protein binding: a critical review of analytical tools, Anal. Bioanal. Chem. 398 (2010) 53–66.

[2] Z. Li, S.R. Beeram, C. Bi, D. Suresh, X. Zheng, D.S. Hage, High-performance affinity chromatography: applications in drug-protein binding studies and personalized medicine, in: R. Donev (Ed.), Advances in Protein Chemistry and Structural Biology, Elsevier, Cambridge, MA, 2016: pp. 1–39.

[3] R. Mallik, M.J. Yoo, C.J. Briscoe, D.S. Hage, Analysis of drug-protein binding by ultrafast affinity chromatography using immobilized human serum albumin, J. Chromatogr. A 1217 (2010) 2796–2803.

[4] X. Zheng, Z. Li, M.I. Podariu, D.S. Hage, Determination of rate constants and equilibrium constants for solution-phase drug-protein interactions by ultrafast affinity extraction, Anal. Chem. 86 (2014) 6454–6460.

[5] S.R. Beeram, X. Zheng, K. Suh, D.S. Hage, Characterization of solution-phase drug-protein interactions by ultrafast affinity extraction, Methods 146 (2018) 46–57.

[6] D.S. Hage, J.D. Carr, Analytical Chemistry and Quantitative Analysis, Prentice Hall, New York, 2011.

[7] S. Iftekhar, D.S. Hage, Evaluation of microcolumn stability in ultrafast affinity extraction for binding and rate studies, J. Chromatogr. B 1187 (2021) 123047.

[8] B. Yang, X. Zheng, D.S. Hage, Binding studies based on ultrafast affinity extraction and single- or two-column systems: interactions of second- and third-generation sulfonylurea drugs with normal or glycated human serum albumin, J. Chromatogr. B 1102–1103 (2018) 8–16.

[9] X. Zheng, M. Podariu, R. Matsuda, D.S. Hage, Analysis of free drug fractions in human

serum by ultrafast affinity extraction and two-dimensional affinity chromatography, Anal. Bioanal. Chem. 408 (2016) 131–140.

[10] S.R. Beeram, C. Zhang, K. Suh, W.A. Clarke, D.S. Hage, Characterization of drug binding with alpha$_1$-acid glycoprotein in clinical samples using ultrafast affinity extraction, J. Chromatogr. A 1649 (2021) 462240.

[11] C. Bi, X. Zheng, D.S. Hage, Analysis of free drug fractions in serum by ultrafast affinity extraction and two-dimensional affinity chromatography using α_1-acid glycoprotein microcolumns, J. Chromatogr. A 1432 (2016) 49–57.